ANTIOXIDANTS & REDOX SIGNALING
Volume 00, Number 00, 2013

DOI: 10.1089/ars.2013.5295

FORUM ORIGINAL RESEARCH COMMUNICATION

Manganese Superoxide Dismutase Is a Promising Target for Enhancing Chemosensitivity of Basal-like Breast Carcinoma

Alan Prem Kumar,[1–4,*] Ser Yue Loo,[1,5,*] Sung Won Shin,[6] Tuan Zea Tan,[1] Chon Boon Eng,[7] Rajeev Singh,[7,8] Thomas Choudary Putti,[9] Chee Wee Ong,[1,10] Manuel Salto-Tellez,[1,9,10] Boon Cher Goh,[1,11] Joo In Park,[6] Jean Paul Thiery,[1,5,12] Shazib Pervaiz,[1,13–16,†] and Marie Veronique Clement[5,13,†]

Abstract

Aims: Although earlier reports highlighted a tumor suppressor role for manganese superoxide dismutase (MnSOD), recent evidence indicates increased expression in a variety of human cancers including aggressive breast carcinoma. In the present article, we hypothesized that MnSOD expression is significantly amplified in the aggressive breast carcinoma basal subtype, and targeting MnSOD could be an attractive strategy for enhancing chemosensitivity of this highly aggressive breast cancer subtype. ***Results:*** Using MDA-MB-231 and BT549 as a model of basal breast cancer cell lines, we show that knockdown of MnSOD decreased the colony-forming ability and sensitized the cells to drug-induced cell death, while drug resistance was associated with increased MnSOD expression. In an attempt to develop a clinically relevant approach to down-regulate MnSOD expression in patients with basal breast carcinoma, we employed activation of the peroxisome proliferator-activated receptor gamma (PPARγ) to repress MnSOD expression; PPARγ activation significantly reduced MnSOD expression, increased chemosensitivity, and inhibited tumor growth. Moreover, as a proof of concept for the clinical use of PPARγ agonists to decrease MnSOD expression, biopsies derived from breast cancer patients who had received synthetic PPARγ ligands as anti-diabetic therapy had significantly reduced MnSOD expression. Finally, we provide evidence to implicate peroxynitrite as the mechanism involved in the increased sensitivity to chemotherapy induced by MnSOD repression. ***Innovation and Conclusion:*** These data provide evidence to link increased MnSOD expression with the aggressive basal breast cancer, and underscore the judicious use of PPARγ ligands for specifically down-regulating MnSOD to increase the chemosensitivity of this subtype of breast carcinoma. *Antioxid. Redox Signal.* 00, 000–000.

[1]Cancer Science Institute of Singapore, National University of Singapore, Singapore, Singapore.
[2]Department of Pharmacology, Yong Loo Lin School of Medicine, National University of Singapore, Singapore, Singapore.
[3]Faculty of Health Sciences, School of Biomedical Sciences, Curtin University, Perth, Western Australia.
[4]Department of Biological Sciences, University of North Texas, Denton, Texas.
[5]Department of Biochemistry, Yong Loo Lin School of Medicine, National University of Singapore, Singapore, Singapore.
[6]Department of Biochemistry, Dong-A University College of Medicine and Medical Research Center for Cancer Molecular Therapy, Dong-A University, Busan, South Korea.
[7]NUH-NUS Tissue Repository, National University Hospital, Singapore, Singapore.
Departments of [8]Surgery and [9]Pathology, Yong Loo Lin School of Medicine, National University of Singapore, Singapore, Singapore.
[10]Centre for Cancer Research and Cell Biology, Queen's University Belfast, Belfast, United Kingdom.
[11]Department of Haematology-Oncology, National University Hospital, Singapore, Singapore.
[12]Institute of Molecular and Cellular Biology, A*Star Singapore, Singapore, Singapore.
[13]NUS Graduate School for Integrative Sciences and Engineering, National University of Singapore, Singapore, Singapore.
[14]Duke-NUS Graduate Medical School, Singapore, Singapore.
[15]Singapore-MIT Alliance, Singapore, Singapore.
[16]Department of Physiology, Yong Loo Lin School of Medicine, National University of Singapore, Singapore, Singapore.
*These authors contributed equally to this work.
†These authors contributed equally to senior authorship.

Innovation

Manganese superoxide dismutase (MnSOD) is a major regulator of cellular redox metabolism. Although earlier reports highlighted a tumor suppressor role for MnSOD, recent evidence indicates increased expression in a variety of human cancers. To that end, our data provide evidence to link increased expression of MnSOD with the aggressive basal subtype of breast cancer, and underscore the judicious use of peroxisome proliferator-activated receptor gamma ligands for specifically down-regulating MnSOD to induce mitochondrial oxidative stress-dependent increase in chemosensitivity of this sub-type of breast cancer with limited treatment options.

Introduction

Breast carcinoma is the most frequently diagnosed malignancy among women in the Western world and the second leading cause of cancer-related deaths in women (21). While considerable progress has been made in the diagnosis and treatment of estrogen-dependent breast cancer with much improved patient survival, estrogen-independent breast cancer, particularly tumors of the basal subtype, are associated with poor prognosis partly due to a lack of target-specific therapeutic options. Therefore, it is highly desirable to identify subtype specific signaling networks and/or molecular mechanisms with the overall objective of designing and developing effective therapeutic strategies.

Among the many aberrations in the regulation of cell growth and fate signaling associated with the process of carcinogenesis or cancer progression is a significant change in the overall cellular metabolism (2, 35, 42). The increases in the energy demand and metabolic activity result in a change in cellular redox milieu, which is further compounded by alterations in the anti-oxidant defense capacity (63, 69). While the reported evidence implicates a reduced anti-oxidant capacity in the initiation of carcinogenesis, the high metabolic flux in the settings of an established tumor may result in a robust induction of cellular anti-oxidant enzymes to cope with the increase in oxidative stress. Along these lines, our recent work has unraveled distinct redox signaling in cancer cell fate decisions (1, 8, 55, 56).

Since mitochondrial respiration is an important source of superoxide (O_2^-) generation in the cells apart from NADPH oxidases, manganese superoxide dismutase (MnSOD) plays an importance role in maintaining redox balance and mitochondrial integrity (49). There is compelling evidence that cancer cells are heavily reliant on the activity of the various SODs (25) to deal with the acquired oxidative stress (23). Of note, while an earlier body of work demonstrated a tumor suppressor function of MnSOD (4, 43, 50), other reports demonstrated significantly higher expression of MnSOD in human tumors than their normal counterparts (9, 27, 39, 51). Not only has MnSOD overexpression been reported in cancers of the thyroid, brain, gastric, and colon (9, 28, 48), but also, more importantly, recent data indicate that in lung, gastric, and liver cancer patients, high MnSOD gene expression correlates with poorer prognosis, lower overall survival rates, and lower relapse-free survival (5, 34, 61).

Interestingly, more recent studies provide a plausible explanation for the high variability in MnSOD gene expression in cancers. The authors show that MnSOD gene expression decreases *in vivo* as cells transit to early-stage cancer, reiterating its tumor suppressor function. However, MnSOD gene expression increases when cells acquire a more aggressive and invasive phenotype, a phenotype that is typically observed in basal subtype of breast tumors (10, 11, 13, 15). Relevant to this study, studies have also reported higher levels of MnSOD expression in invasive basal-like breast cancer cell lines (MDA-MB-231 and BT-549), compared with the noninvasive (MCF-7 and T47D) or nontumorigenic cell lines (MCF-12A and MCF-12F) (33, 47). These data provide testimony that targeting MnSOD could be an attractive therapeutic strategy against basal-type breast tumors, which would render cells susceptible to oxidative stress-induced cell death. To that end, increased mitochondrial reactive oxygen species (MitoROS) generation has been proposed as an effective anti-cancer strategy (54, 68).

We recently reported that the human MnSOD promoter region contains peroxisome proliferator response element (PPRE) binding motifs and that activation of the peroxisome proliferator-activated receptor-γ (PPARγ) in invasive basal-like breast cancer cells (MDA-MB-231 and MDA-MB-468) resulted in a significant decrease in MnSOD mRNA and protein levels (64). We and others have previously shown that breast cancer cells express higher levels of PPARγ compared with normal breast epithelial cells (14, 37, 40), and that PPARγ activation inhibited proliferation of liposarcoma (62), breast adenocarcinoma (14, 37, 40), prostate carcinoma (36), and colorectal carcinoma (12). Furthermore, ligand activation of PPARγ produces ROS that play critical roles in regulating cell proliferation, apoptosis, and transformation. Thus, upsetting the intracellular ROS balance to activate apoptotic pathways is closely associated with PPARγ-induced cytotoxicity. However, the mechanism(s) by which PPARγ agonism induces ROS production were never clearly elucidated. Several possible mechanisms are suggested in Table 1, but none of these has been experimentally proven. Since MnSOD is a direct target of PPARγ, we hypothesize that repression of MnSOD accounts for the known changes in intracellular ROS levels in tumor cells treated with PPARγ ligands.

Here, we provide evidence *in vitro* and *in vivo* that activation of PPARγ induces tumor-specific down-regulation of MnSOD in basal sub-type of breast cancer, which significantly increases chemosensitivity *via* an increase in intracellular ROS. These findings suggest a novel way to exploit the use of synthetic agonists of PPARγ for the selective targeting of MnSOD in combination with ROS-producing drugs in a unique antitumor strategy against basal breast carcinoma coined "*tumor-specific oxidative stress therapy*."

Results

MnSOD expression is significantly higher in the basal-like and claudin-low breast carcinoma subtypes

Taking advantage of publicly available microarray data, we assessed the expression of MnSOD in relation to the subtype of breast carcinoma. Five hundred and thirty six invasive ductal breast carcinomas microarray profiles were downloaded from The Cancer Genome Atlas (TCGA). The subtypes of these 536 breast cancer tumors were then predicted using

Table 1. ROS Production Induced by PPARγ Ligands in Human Cell Lines

	PPARγ ligand	Concentration	Type of free radicals	Probe used	Suggested mechanism proposed for ROS production	Cell type	Source
1	15d-PGJ_2	1–10 μM	$^{\bullet}OH$, $O_2^{\bullet -}$	Carboxy-H_2DCFDA, Lucigenin	Activation of xanthine oxidase	Lymphocytes	(3)
2	15d-PGJ_2, PGD_2, Rosiglitazone, Ciglitazone Troglitazone	8 μM 20 μM	H_2O_2, $ONOO^-$, $^{\bullet}OH$	Carboxy-H_2DCFDA	Nucleophilic addition reactions with thiols	Leukemic cells	(6)
3	15d-PGJ_2	2.5 μM	H_2O_2, $ONOO^-$, $^{\bullet}OH$, $O_2^{\bullet -}$	Carboxy-H_2DCFDA; MitoSOX Red	Not reported	B lymphocytes	(58)
4	Troglitazone, Ciglitazone	10–100 μM	H_2O_2	Carboxy-H_2DCFDA	Inhibition of mitochondria complex I & II	Jurkat T cells	(60)
5	Ciglitazone	20 μM	H_2O_2, $ONOO^-$, $^{\bullet}OH$	Carboxy-H_2DCFDA	Mitochondrial depolarization	Glioma cells	(30)
6	15d-PGJ_2	1–30 μM	H_2O_2, $ONOO^-$, $^{\bullet}OH$	Carboxy-H_2DCFDA	Disruption of mitochondrial membrane potential	Osteoblastic cells	(41)
7	15d-PGJ_2	5–20 μM	H_2O_2, $ONOO^-$, $^{\bullet}OH$	Carboxy-H_2DCFDA	NADPH activation,	Leukemic cells, colorectal cancer cells	(59)
8	Ciglitazone	10 μM	H_2O_2, $ONOO^-$, $^{\bullet}OH$	Carboxy-H_2DCFDA	Not reported	Renal cells	(38)

ROS, reactive oxygen species; PPARγ, peroxisome proliferator-activated receptor gamma.

Single-Sample Geneset Enrichment Analysis (ssGSEA; Verhaak *et al.*[65]) and breast cancer subtype signature (57). Interestingly, when comparing each subtype against the others, the mean MnSOD expression was significantly higher in the basal and claudin-low breast carcinoma subtypes (Mann-Whitney test, $p = 8.93e\text{-}20$ and $p = 1.3e\text{-}7$, respectively), whereas the mean MnSOD expression was significantly lower in Luminal A and B subtypes (Mann–Whitney test, $p = 6.8e\text{-}13$, and $p = 6.5e\text{-}4$ respectively) (comparing each luminal subtype against the other subtypes) (Fig. 1A). Of note, an identical pattern of expression for MnSOD was observed using a second collection of 3992 breast carcinomas on Affymetrix U133a or U133 Plus2 platform collated from Gene Expression Omnibus (GEO) database (Fig. 1B); a binary comparison of mean MnSOD expression values in each subtype against others revealed that basal, claudin-low, and ERBB2 subtypes have significantly higher expression levels (Mann–Whitney test, $p = 2.95e\text{-}128$, $p = 2.33e\text{-}22$, and $p = 1.41e\text{-}31$, respectively) compared with luminal A, luminal B, and normal-like subtypes; whereas the mean expression was significantly lower in Luminal A and Luminal B subtypes (Mann–Whitney test, $p = 4.53e\text{-}76$, and $p = 7.56e\text{-}37$, respectively) compared against the other subtypes.

High MnSOD expression correlates with poor survival in the basal subtype

Intrigued by the higher MnSOD expression in the basal subtype of cancers using two independent datasets, we set out to investigate whether a higher MnSOD expression could be a poor prognostic indicator in this particular subtype of breast carcinoma. To do so, we analyzed the association of MnSOD gene expression level with survival of patients within the basal breast tumor subtype over a period of 90 months ($\sim$7.5 years). Kaplan–Meier analysis on 72 basal-like breast cancer patients with available survival information from the TCGA database was performed. In this Kaplan–Meier analysis, patients within the basal subtype were classified into MnSOD-high or -low group based on the median of MnSOD expression levels (Fig. 1C). Subsequently, the survival curves for the MnSOD-high and MnSOD-low groups were compared. Although there was no significant difference in terms of p-value, due to the relatively small number of samples, a separation in survival curves was observed between the MnSOD-high and -low groups (log-rank test, $p = 0.2792$; hazard ratio = 0.4404). Hence, this result strongly supports the fact that low MnSOD expression in patients with basal breast cancer type could have a better survival as compared with those in the MnSOD-high group (Fig. 1C).

Down-regulation of MnSOD enhances chemosensitivity of basal-like breast carcinoma cell lines

Based on our data suggesting a relatively poorer prognosis for the patients in the high MnSOD group within the basal subtype of breast cancers, we hypothesize that MnSOD could be an attractive therapeutic target in the management of this particular subtype of tumor. To test this hypothesis, we used two human breast cancer cell lines (MDA-MB-231 and BT549) that were recently shown to closely resemble the clinical basal-like tumors (32). Our results show that gene knockdown of MnSOD using specific small-interfering ribonucleic acid (siRNA) impaired

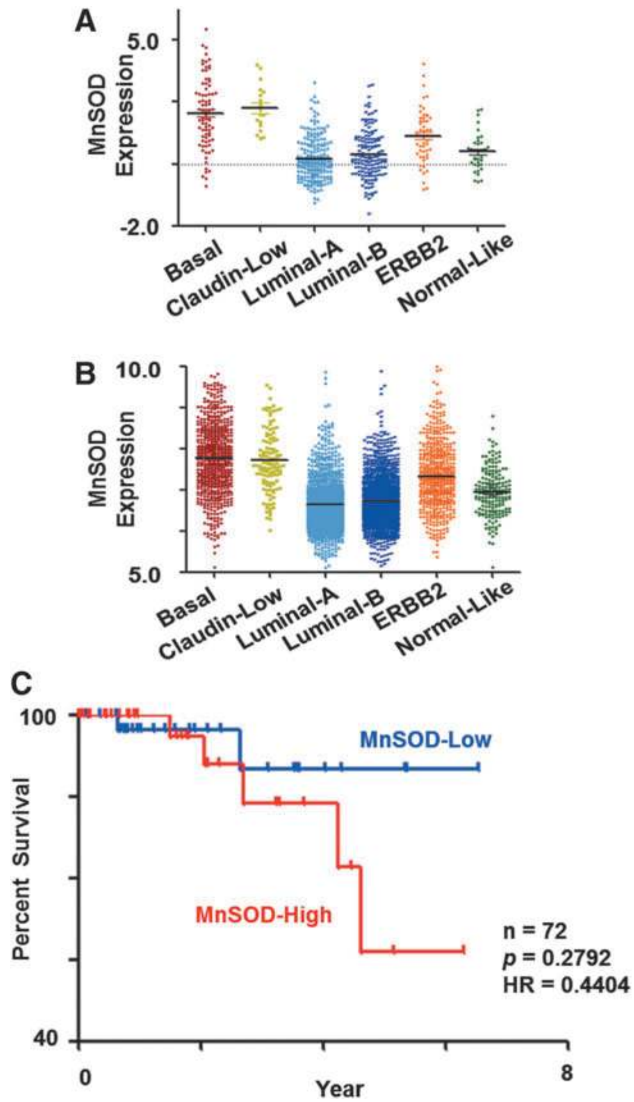

FIG. 1. Low manganese superoxide dismutase (MnSOD) expression in breast cancer patients translates into higher survival rates. **(A)** MnSOD gene expression among 536 breast cancer patient data from The Cancer Genome Atlas. Dot plot of MnSOD gene expression value (y-axis) for each breast cancer subtype, namely Basal, Claudin-low, Luminal-A, Luminal-B, ERBB2 (HER2+), and Normal like. Maroon color represents basal subtype; yellow represents Claudin-low subtype; light blue represents Luminal-A, whereas dark blue represents Luminal-B tumors. ERBB2 and Normal-like tumors are represented by orange and green, respectively. **(B)** MnSOD gene expression among 3992 breast cancer patient data from Affymetrix platform. Dot plot of MnSOD gene expression value (y-axis) for each breast cancer subtype, namely Basal, Claudin-low, Luminal-A, Luminal-B, ERBB2 (HER2+), and Normal like. Maroon color represents basal subtype; yellow represents Claudin-low subtype; light blue represents Luminal-A, whereas dark blue represents Luminal-B tumors. ERBB2 and Normal-like tumors are represented by orange, and green, respectively. **(C)** Kaplan–Meier plot of MnSOD-high and -low groups defined by median of MnSOD expression in patients within the basal subtype ($n = 72$). Log-rank test was used to compute the *p*-value. Low expression of MnSOD is represented by blue, whereas high expression of MnSOD is represented by red. Abbreviation: HR, Hazard Ratio. To see this illustration in color, the reader is referred to the web version of this article at www.liebertpub.com/ars

long-term colony-forming ability (Fig. 2A, B and Supplementary Fig. S1A, B; Supplementary Data are available online at www.liebertpub.com/ars) as well as significantly increased the sensitivity of both cell lines to docetaxel (DOC) and doxorubicin (DOX) (Fig. 2C–G and Supplementary Fig. S1C–E), two commonly used drugs for the treatment of breast cancer. An MnSOD activity assay was performed to validate that changes in MnSOD protein expression corresponded to changes in protein activity (Supplementary Fig. S9A, B). Manipulation of MnSOD was also found to change reduced/oxidized glutathione (GSH/GSSG) ratios accordingly but had no significant effects on catalase expression (Supplementary Fig. S9C–F).

PPARγ activation down-regulates MnSOD expression in basal-like breast carcinoma cell lines

Our results so far indicated that targeting MnSOD expression could have potential implications in enhancing the chemosensitivity of basal-like subtype of breast tumors. However, for this approach to have therapeutic applications, there is a need to find a clinically relevant protocol to selectively decrease MnSOD expression in these cells. Interestingly, we recently showed that human MnSOD gene is a target of the PPARγ. A functional PPRE was identified in the upstream/promoter region of the human MnSOD gene. Of note, activation of PPARγ by its endogenous ligand, 15-deoxy $^{\Delta 12,14}$-PGJ$_2$ (15d-PGJ$_2$), significantly decreased MnSOD promoter activity and mRNA level in the basal-like tumor cell lines MDA-MB-231 and MDA-MB-468 (64). In the present article, these results were reproduced using BT549 cells and confirmed in the MDA-MB-231 cell line. Exposure of MDA-MB-231 and BT549 cells to 15d-PGJ$_2$ induced the activation of PPARγ (Supplementary Fig. S2A), which correlated with a dose-dependent decrease in MnSOD mRNA level and protein expression (Fig. 3A, B and Supplementary Fig. S2B, C). Moreover, the down-regulation of MnSOD mRNA and protein expression with 15d-PGJ$_2$ was inhibited by the selective and irreversible PPARγ antagonist GW9662 (Fig. 3A, B, Supplementary Fig. S2B, C) or on transfection of the cells with a dominant negative form of PPARγ, PPAR$\gamma^{C126A/E127A}$ (Fig. 3C and Supplementary Fig. S2D). On the contrary, exposure of the nontumorigenic breast cell lines 184A1 and MCF10A to 15d-PGJ$_2$ neither induced PPARγ activation nor resulted in a decrease in MnSOD mRNA and/or protein expression (Supplementary Figs. S2A and S3A, B).

Next, to assess whether down-regulation of MnSOD was associated with the inhibitory effect of PPARγ activation on tumor growth, viable MDA-MB-231 cells were injected into the mammary fat pads of 6 week-old female Balb/c nude mice. Tumors were allowed to grow to a volume of 50–70 mm^3 before the tumor-bearing mice were separated into a control and a 15d-PGJ$_2$–treated group. As shown in Figure 3D, administration of 15d-PGJ$_2$ given at a dose of 5 mg/kg *via* tail vein every 3 days significantly inhibited further tumor growth; the mean tumor volume in the 15d-PGJ$_2$ group was significantly smaller than the vehicle-treated control group (control group mean = 131.55 ± 6.16 mm^3; 15d-PGJ$_2$ group mean = 56.62 ± 11.28 mm^3). Most importantly, not only did 15d-PGJ$_2$ induce activation of PPARγ *in vivo*, but also a significant down-regulation of MnSOD expression was detected in the 15d-PGJ$_2$ group (Fig. 3E).

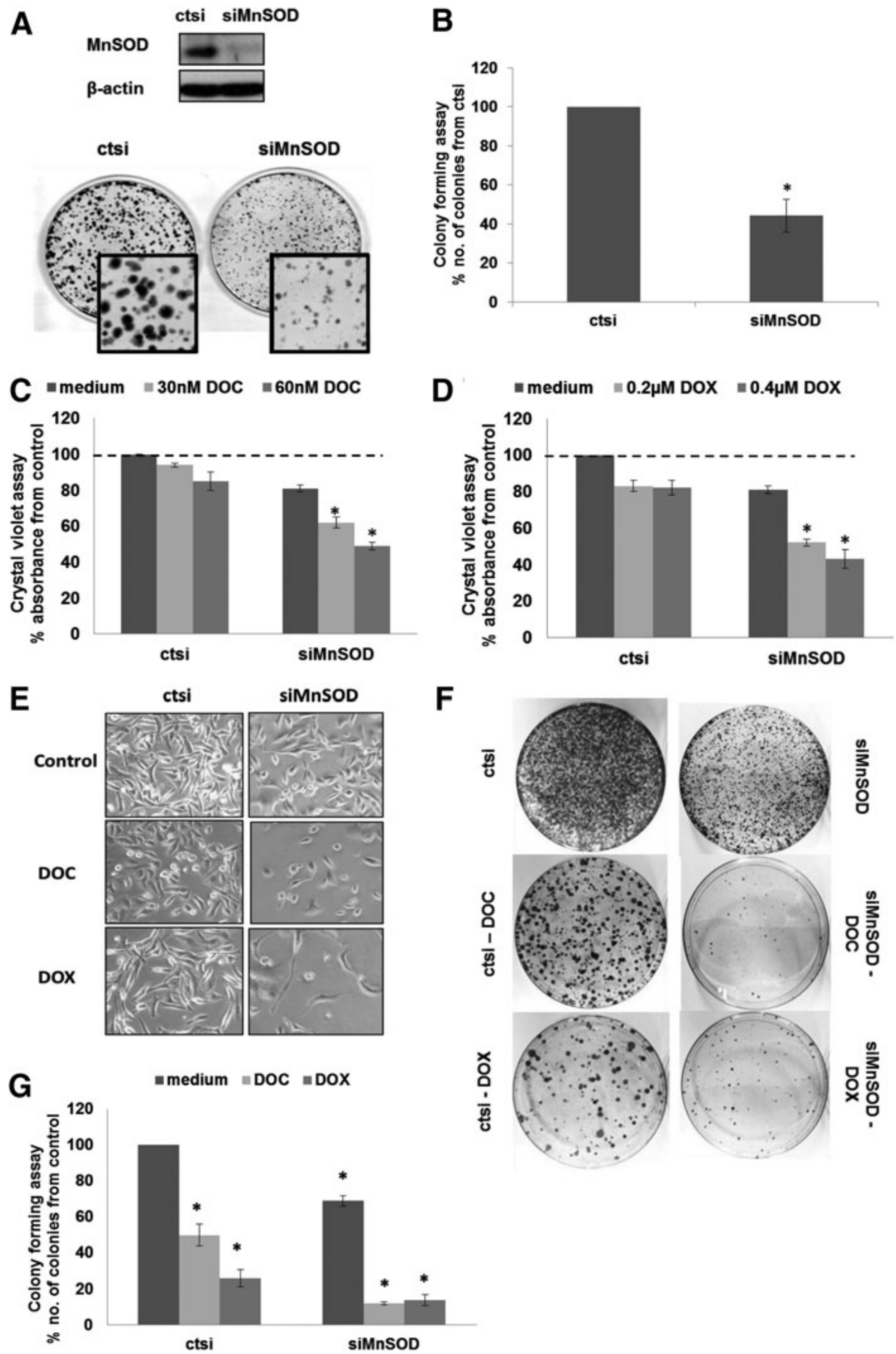

FIG. 2. Targeted repression of MnSOD inhibits colony-forming ability of basal-like breast tumor cells and increases sensitivity to chemotherapeutic drugs. (A) *Top panel*: Western blot of MDA-MB-231 cells transfected with 100 n*M* control scrambled siRNA (ctsi) and siMnSOD. *Bottom panel*: Colony-forming assay of MDA-MB-231 cells transfected with ctsi and siMnSOD and grown for 2 weeks. **(B)** Number of colonies from **(A)** was counted. Results shown represent mean ± SD, $n=3$, *$p<0.05$ *versus* ctsi. **(C)** MDA-MB-231 cells were transfected with ctsi and siMnSOD. Forty eight hours post transfection, cells were treated with 30 and 60 n*M* docetaxel (DOC) for 48 h before cell viability was assessed using crystal violet assay. **(D)** MDA-MB-231 cells were transfected with ctsi and siMnSOD. Forty eight hours post transfection, cells were treated with 0.2 and 0.4 μM doxorubicin (DOX) for 48 h before cell number was assessed using crystal violet assay. Results shown represent mean ± SD, $n=3$, *$p<0.05$ *versus* control. **(E)** Light microscopy images of MDA-MB-231 cells transfected with ctsi and siMnSOD and treated with 60 n*M* DOC or 0.4 μM DOX for 48 h (×200 magnification). **(F)** Colony-forming assay of MDA-MB-231 cells transfected with ctsi and siMnSOD and treated with 60 n*M* DOC or 0.4 μM DOX for 48 h. Cells were re-seeded and grown for 2 weeks. **(G)** Number of colonies from **(F)** was counted. Results shown represent mean ± SD, $n=3$, *$p<0.05$ *versus* ctsi.

Having demonstrated that activation of PPARγ using its natural ligand 15d-PGJ$_2$, specifically decreased MnSOD expression in basal breast cancer cell lines and a xenograft model, we next investigated whether these results could be reproduced using synthetic PPARγ ligands, such as rosiglitazone and troglitazone. MDA-MB-231 and BT549 cells were exposed to increasing concentrations of rosiglitazone and troglitazone to determine the concentration required to detect an activation of PPARγ. Exposure of MDA-MB-231 to 40 to 80 μM rosiglitazone and 30 to 50 μM troglitazone induced significant increases in PPARγ activation (Supplementary Fig. S4A, B) that were prevented in the presence of the PPARγ antagonist GW9662. Moreover, a down-regulation of MnSOD mRNA level and protein expression that was inhibited by GW9662 was also observed (Fig. 4A–D).

Validation of PPAR-γ-mediated repression of MnSOD in patient-derived breast cancer tissue

In order to provide a "proof of concept" that synthetic PPARγ ligands could induce a decrease in MnSOD expression in the clinical setting, we exploited the therapeutic use of the synthetic PPARγ ligands for the management of type 2

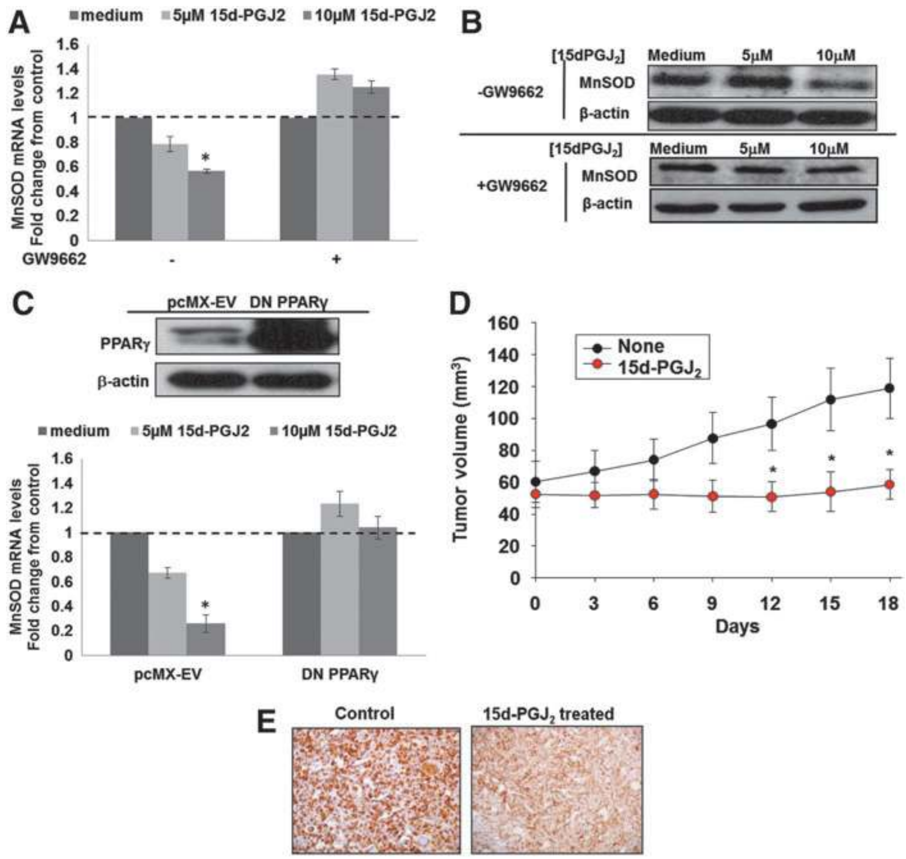

FIG. 3. Activation of peroxisome proliferator-activated receptor gamma (PPARγ) down-regulates MnSOD expression in the MDA-MB-231 breast carcinoma cell line. (A) Real-time Polymerase Chain Reaction (RT-PCR) analysis of relative MnSOD mRNA levels normalized to 18S mRNA levels. MDA-MB-231 cells were subjected to 24 h of 5 and 10 μM 15-deoxy $^{\Delta 12,14}$-PGJ$_2$ (15d-PGJ$_2$) treatment with and without 4 h preincubation with 10 μM GW9662. Results are expressed as fold changes from control. Results shown represent mean $\pm$ SD, $n = 4$, $*p < 0.05$ *versus* control. **(B)** Western blot analysis of MDA-MB-231 breast cancer cells $\pm$ GW9662 preincubation and then treated with 5 and 10 μM 15d-PGJ$_2$ for 24 h. **(C)** *Top panel*: Western blot analysis of MDA-MB-231 cells transfected with pcMX-EV and 5 μg DNPPARγ (plasmids encoding a dominant negative form of PPARγ). *Bottom panel*: RT-PCR analysis of relative MnSOD mRNA levels normalized to 18S mRNA levels in MDA-MB-231 cells transfected with DNPPARγ or pcMX-EV before exposure to increasing doses of 15d-PGJ$_2$ for 24 h. Results are expressed as fold changes from control. Results shown represent mean $\pm$ SD, $n = 3$, $*p < 0.05$ *versus* control. **(D)** MDA-MB-231 cells (1×10^7 cells/100 μl) were inoculated in the mammary fat pads of female Balb/c nude mice. Once the tumor volume reached 50 to 70 mm^3, mice were randomized into two groups ($n = 3$), and treatment was initiated. Mice were treated with vehicle control and 15d-PGJ$_2$ (5 mg/kg) as described in "Materials and Methods." Tumor size was measured daily with a caliper (calculated volume = shortest diameter^2 $\times$ longest diameter/2). $*p < 0.05$, significantly different from respective control. Serum levels of glutamate-oxaloacetate transaminase and glutamate-pyruvate transaminase were assessed to monitor organ toxicity in animals receiving 15d-PGJ$_2$, and the dosage used in the *in vivo* study was safe based on these parameters, as previously reported (59). **(E)** Tumor tissues obtained from experiment described earlier on day 18 were subjected to immunohistochemistry using antibodies against MnSOD. The sections were counterstained with hematoxylin and photographed with a Scan Scope (Aperio Technologies, Inc.). To see this illustration in color, the reader is referred to the web version of this article at www.liebertpub.com/ars

Diabetes Mellitus. To that end, we compared the expression of MnSOD in breast cancer tissues of diabetic patients treated with rosiglitazone *versus* breast cancer patients who did not receive rosiglitazone (but other anti-diabetic drugs) for their diabetic condition and/or nondiabetic patients with breast cancer. A total of 15 cases of carcinoma of the breast (intra-ductal carcinoma grade 2 to grade 3) with available paraffin-embedded tissue blocks were identified for the period 2004 and 2006 from the pathology files of the Department of Pathology, National University of Singapore. These cases were divided into three groups: Group I: diabetic breast cancer patients treated with rosiglitazone, Group II: diabetic breast cancer patients treated with other anti-diabetic drugs, and Group III: nondiabetic breast cancer patients. Immunohistochemical (IHC) analysis showed that the expression of MnSOD in clinical tissues corroborated our findings in breast cancer cell lines on the repressive effect of PPARγ activation on MnSOD expression: three out of four patients in Group I (diabetics on rosiglitazone) showed reduced levels of MnSOD expression compared with the tumors of all patients from the other two groups. Note that the invasive ductal carcinoma grade at diagnosis was similar within the different groups (Fig. 4E). A representative immunohistochemistry stain of a tumor tissue

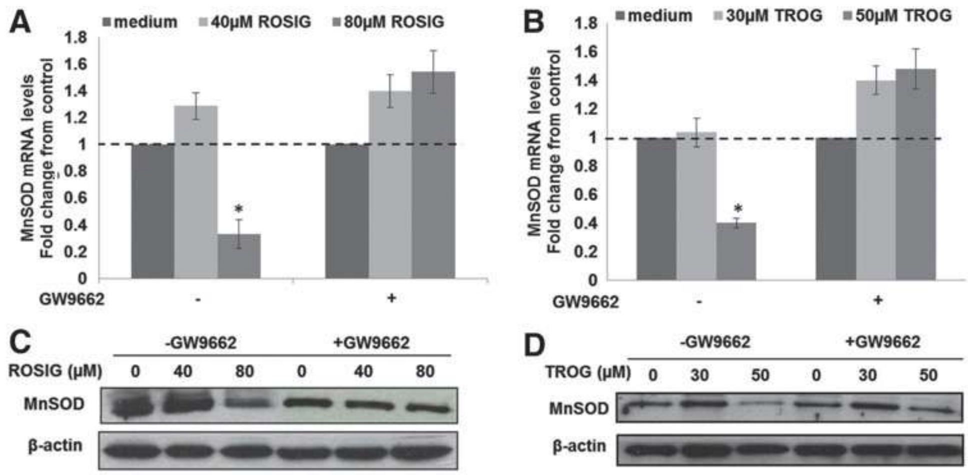

	MnSOD (IHC) Scoring	Tumour	Normal
	Breast cases		
Group I - On Rosiglitazone	Case1	0	2+
	Case2	0	2+
	Case3	2+	NA
	Case4	0	2+
Group II - On other antidiabetics	Case5	2+	3+
	Case6	1+	2+
	Case7	2+	3+
	Case8	2+	2+
	Case9	2+	1+
	Case10	2+	2+
Group III - Non diabetics	Case11	2+	2+
	Case12	2+	2+
	Case13	3+	2+
	Case14	2+	2+
	Case15	2+	2+
	Case16	2+	2+

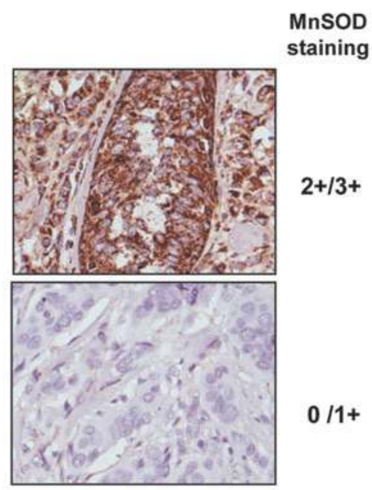

FIG. 4. Synthetic glitazones repress MnSOD expressions in breast tumor cell lines and in tissues from breast cancer patients on rosiglitazone treatment. (A) MDA-MB-231 ± GW9662 were treated with 40 and 80 μM rosiglitazone for 24 h. RT-PCR analysis of relative MnSOD mRNA levels normalized to 18S mRNA levels. Results are expressed as fold changes from control. Results shown represent mean ± SD, $n = 4$, $^*p < 0.05$ *versus* control. **(B)** MDA-MB-231 ± GW9662 were treated with 30 and 50 μM troglitazone for 24 h. RT-PCR analysis of relative MnSOD mRNA levels normalized to 18S mRNA levels. Results are expressed as fold changes from control. Results shown represent mean ± SD, $n = 3$, $^*p < 0.05$ *versus* control. **(C)** Western blot analysis of MDA-MB-231 ± GW9662 and treated with 40 and 80 μM rosiglitazone for 24 h. **(D)** Western blot analysis of MDA-MB-231 ± GW9662 and treated with 30 and 50 μM troglitazone. **(E)** *Left panel*: Immunohistochemical (IHC) MnSOD scoring results for breast cancer tissues and matched normal tissues from three different groups of patients: (Group I) diabetic breast cancer patients treated with rosiglitazone; (Group II) diabetic breast cancer patients treated with other anti-diabetic drugs; and (Group III) nondiabetic breast cancer patients. *Right panel*: IHC localization of MnSOD antigen done on formalin-fixed, paraffin-embedded tumor breast tissues. Tissue sections were incubated with rabbit monoclonal MnSOD antibody. Positively stained cells were evaluated using the following intensity categories: 0 (no staining), 1 + (weak but detectable staining), 2 + (moderately intense staining), and 3 + (very intense staining) (×20 magnification). To see this illustration in color, the reader is referred to the web version of this article at www.liebertpub.com/ars

(2 + /3 +) showing higher MnSOD expressions than a tumor tissue (0/1 +) is presented on the right panel of Figure 4E.

MnSOD regulates PPARγ activation-induced chemosensitization of MDA-MB-231 cells

Synthetic ligands of PPARγ have been shown to sensitize a variety of human cancer cell types to chemotherapy-induced cell death. Intrigued by our findings that gene knockdown of MnSOD enhanced chemosensitivity of MDA-MB-231 cells (Fig. 2C–G) and activation of PPARγ down-regulated MnSOD expression (Fig. 3A, B), we questioned whether the chemosensitizing effect of PPARγ ligands could be mediated *via* their repressive effect on MnSOD. Indeed, exposure of MDA-MB-231 cells to rosiglitazone alone or in combination with DOC or DOX resulted in a significant down-regulation of MnSOD expression (Fig. 5A), and the combination treatment drastically affected the clonogenic potential of these basal-like breast cancer cells (Fig. 5B–D). Most importantly, the chemosensitizing effect of rosiglitazone was significantly blocked on overexpression of MnSOD (Fig. 5E–I), thus providing further testimony for a critical role of MnSOD in regulating the chemosensitizing effect of PPARγ activation. Similar treatment of nontumorigenic cells (MCF10A and 184A1) had negligible effects on MnSOD expression and cell survival, thus providing further evidence that this effect is specific to cancer cells (Supplementary Figs. S5A–F, S6A–H).

Validation of MnSOD as a potential target in chemotherapy-resistant breast cancer

Acquisition of chemoresistance remains a major challenge in the therapeutic management of breast cancer. Based on our data demonstrating the ability of MnSOD to block death signaling in breast cancer cells, we set out to generate chemotherapy resistant clones of MDA-MB-231 cell line and assessed the role of MnSOD. This was accomplished by exposing cells to DOX or DOC in a 'stepwise increase' method for a period of 4–6 weeks and selecting the surviving clones (Fig. 6A, B). Interestingly, the expression of MnSOD (mRNA and protein) was significantly increased in MDA-MB-231 cells that were rendered resistant to both the chemotherapy agents compared with the original MDA-MB-231 cell line (Fig. 6C–F). Furthermore, knockdown of MnSOD using gene-specific siRNA restored the sensitivity of the DOX and DOC MDA-MB231-resistant cell lines, MDA-MB-231 DOX-R and MDA-MB-231 DOC-R, respectively (Fig. 6G, H). Similarly, repression of MnSOD on ligand-induced activation of PPARγ restored chemosensitivity of the drug-resistant variants of MDA-MB-231 (Fig. 6I, J).

MnSOD-targeted chemosensitivity is linked to an accumulation of peroxynitrite

Finally, we set out to understand the mechanism involved in the decrease in viability of basal breast cancer cells and their increased chemosensitivity after down-regulation of MnSOD. Results show that down-regulation of MnSOD expression using siMnSOD or 15d-PGJ$_2$ increases MitoROS as measured by the MitoSOX fluorescent probe. The increase in MitoROS caused by PPARγ activation could be inhibited by N-Acetyl cysteine (NAC) (Fig. 7A, B and Supplementary Fig. S7A, B), overexpression of MnSOD (Fig. 7C–E and Supplementary Fig. S7C), or preincubation with the PPARγ antagonist GW9662 (Fig. 7F–H and Supplementary Fig. S7D).

Since intracellular increase in ROS has been implicated in the anti-cancer activity of DOC or DOX (26, 68), we questioned whether the increased sensitivity of cancer cells to these drugs in combination with PPARγ ligands could be due to this accentuated mitochondrial oxidative stress. Indeed, MitoROS level measured by MitoSOX was further increased in MDA-MB-231 cells on combination treatment with rosiglitazone and DOX or DOC, compared with single agent treatment (Fig. 8A, B). Ectopic overexpression of MnSOD prevented rosiglitazone-induced increase in MitoROS and sensitization to DOC or DOX in MDA-MB-231 cells (Fig. 8C–E), whereas similar treatment of the nontumorigenic cell lines (MCF10A and 184A1) did not significantly alter intracellular ROS levels assayed by MitoSOX (Supplementary Fig. S8A–D).

Accumulation of O_2^- in the mitochondria was confirmed by showing that on treatment with rosiglitazone, DOC or DOX, tiron, but not catalase, could prevent the increase in MitoSOX fluorescence (Fig. 9D–I). Interestingly, in addition to O_2^- production, mitochondria have also been shown to produce the reactive nitrogen species, nitric oxide (NO) (20). Using 4-amino-5-methyamino-2,7′-difluorofluorescein (DAF-FM) to detect NO, our data show that in addition to an increase in O_2^-, an increase in NO level could be detected on silencing of MnSOD in MDA-MB-231 cells (Fig. 9A). NO level was also significantly increased on combination treatment with rosiglitazone and DOC or DOX compared with single-agent treatment (Fig. 9B, C). These data led us to hypothesize that mitochondrial O_2^- production induced by MnSOD repression could react with NO to form the reactive nitrogen species, peroxynitrite ($ONOO^-$), which could be responsible for the enhanced sensitivity to DOC or DOX (52). In agreement with this idea, chemosensitization to DOC or DOX by rosiglitazone was prevented by preincubation of the cells with NAC, Tiron, and the $ONOO^-$ decomposition catalyst, 5,10,15,20-Tetrakis(4-sulfonatophenyl)porphyrinato Iron (III), Chloride (FeTPPS), but not catalase (Fig. 10A–H). Taken together, these data indicate that $ONOO^-$ could be the probable species involved in mitigating enhanced chemosensitivity of basal-like breast carcinoma on gene knockdown or pharmacological inhibition of MnSOD (Fig. 10I).

Discussion

MnSOD expression is associated with aggressive sub-type of breast cancer

We report here, using hierarchical clustering of microarray data, that MnSOD expression was significantly different in the various subtypes of breast carcinoma. The Luminal breast

FIG. 5. Combination of PPARγ ligand and chemotherapeutic drugs decreases cell viability: MnSOD overexpression prevented these effects. (A) *Top panel*: Western blot for MnSOD expression in MDA-MB-231 cells treated with 80 μM rosiglitazone alone, 60 n*M* DOC alone, and in combination for 48 h. *Bottom panel*: Western blot for MnSOD expression in MDA-MB-231 cells treated with 80 μM rosiglitazone alone, 0.4 μM DOX alone, and in combination for 48 h. **(B)** Colony formation in soft agar of MDA-MB-231 cells treated with rosiglitazone alone, DOC alone, DOX alone, combination of rosiglitazone, and DOC or combination of rosiglitazone and DOX respectively. **(C)** Colonies from **(B)** were counted for rosiglitazone alone, DOC alone, and combination of rosiglitazone and DOC and presented as a percentage of control cells, $n=3$, $*p<0.05$ *versus* control. **(D)** Colonies from **(B)** were counted for rosiglitazone alone, DOX alone, and combination of rosiglitazone and DOX and presented as a percentage of control cells, $n=3$, $*p<0.05$ *versus* control. **(E)** Western blot for MDA-MB-231 cells transfected with empty vector pcDNA3 or 2 μg MnSOD plasmid. **(F)** Transfected MDA-MB-231 cells from **(E)** were treated with 80 μM rosiglitazone, 60 n*M* DOC, or both for 48 h and cell viability was assessed by crystal violet assay. **(G)** Transfected MDA-MB-231 cells from **(E)** were treated with 80 μM rosiglitazone, 0.4 μM DOX, or both for 48 h, and cell number was assessed by crystal violet assay. Results shown represent mean ± SD, $n=3$, $*p<0.05$ *versus* control. **(H, I)** Light microscopy images of MDA-MB-231 cells from **(F, G)** under 200× magnification.

carcinoma subtype associated with the less aggressive ER+ breast cancer phenotype had a significantly lower MnSOD expression than the Basal/Claudin-low breast carcinoma subtype that is often associated with the more aggressive ER- breast cancer phenotype.

Evidence from a host of earlier studies suggested a tumor suppressor role for MnSOD; however, the fact that MnSOD is overexpressed in a variety of cancers such as thyroid tumors, neuroblastomas, gastric and colorectal carcinomas (9, 28, 48) argues in favor of a complex

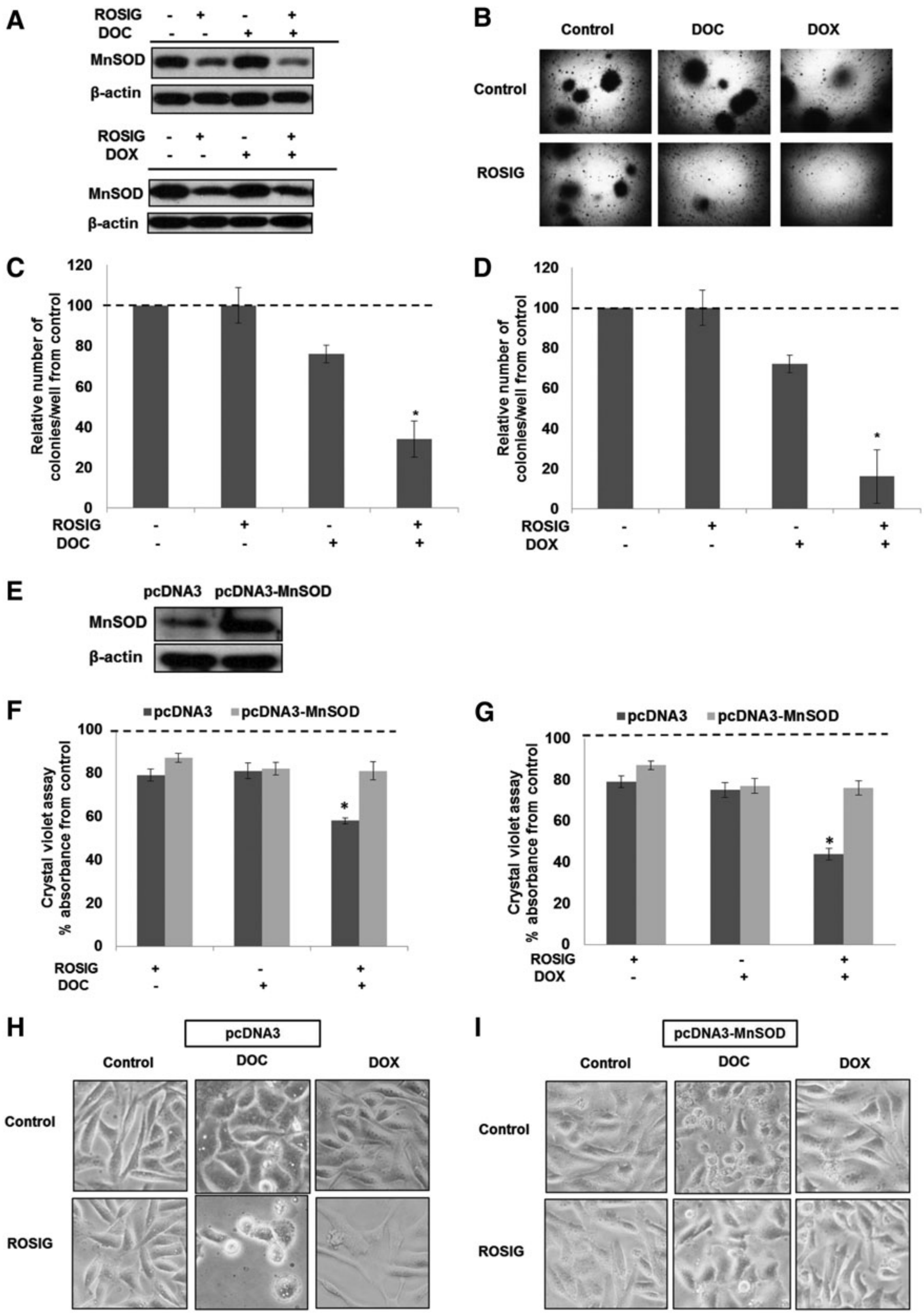

functional biology of this protein in the various stages of cancer development and progression. Moreover, studies reported elevated levels of MnSOD in estrogen-independent breast cancer cell lines, MDA-MB-231 and BT-549, compared with estrogen-dependent, MCF-7 and T47D and nontumorigenic cell lines, MCF-12A and MCF-12F (33, 47). Hence, the correlation between MnSOD expression and tumor aggressiveness suggests the possibility of distinctly different expression patterns for the anti-oxidant gene depending on the stage of the tumor. This dual role of MnSOD was recently demonstrated in a model of skin carcinogenesis in which MnSOD expression was suppressed at a very early stage but increased at a later stage of the skin carcinoma (11). It is plausible that, similar to the development of skin carcinoma, MnSOD may be involved in the suppression of the early development of breast cancer but an increase in MnSOD expression is required for the acquisition of a more aggressive phenotype. Therefore, therapeutic strategies targeting MnSOD may need to be tailored in a subtype-specific manner. For example, the Luminal subtype might be sensitive to an increase in MnSOD expression while Basal and Claudin-low could be more susceptible to a decrease in MnSOD expression. This is further reinforced by the clinical outcomes data demonstrating that patients from the MnSOD-low group within the basal-like subtype may have a better survival than patients in the MnSOD-high group. These data provide impetus to the idea that within the basal carcinoma subtype, MnSOD expression could be a prognostic marker for poor survival. Indeed, supporting the critical role of MnSOD expression in the survival of Basal breast carcinoma and in agreement with a previous report (33), silencing of MnSOD using gene-specific siRNA was associated with a decrease in the colony-forming ability of MBA-MD-231 and BT549 cell lines. Interestingly, a previous study showed that the expression of MnSOD was an important factor in the response of gastric cancer cells to 5-flurouracil (26). In agreement with this article, we observed a significant increase in the basal MnSOD expression in breast cancer cells that were rendered resistant to DOX, and, more importantly, repression of MnSOD restored chemosensitivity in the resistant cells.

PPARγ activation: a promising approach to down-regulate MnSOD expression in basal breast carcinoma

Intrigued by our findings linking MnSOD expression to chemo-resistance, we set out to search for a clinically relevant approach to specifically decrease MnSOD expression in our model cell lines of basal breast carcinoma. To that end, we recently reported the presence of three putative PPREs (24) in the human MnSOD promoter and provided experimental evidence that human MnSOD was, indeed, a PPARγ target gene (64). Of note, among the three PPAR isoforms, PPARγ activation has been shown to inhibit the proliferation of malignant cells from different lineages such as liposarcoma (62), breast adenocarcinoma (14, 37, 40), prostate carcinoma (36), and colorectal carcinoma (12). Here, we present evidence that activation of PPARγ, either *via* its physiological ligand or on exposure to the synthetic ligands, resulted in repression of MnSOD in the basal type breast cancer cell lines (MDA-MB-231 and BT-549) *in vitro* as well as in a MDA-MB-231 xenograft model. Moreover, as a "*proof of concept*" using a cohort of diabetic patients treated with rosiglitazone, we established that rosiglitazone treatment correlated with a low level of MnSOD expression in the breast tumors of diabetic patients treated with rosiglitazone. These data provide strong evidence that the repression of MnSOD by PPARγ activation occurs not only *in vitro*, but also *in vivo*. Similarly, PPARγ activation-induced decrease in MnSOD significantly increased chemosensitivity of the two breast cancer cell lines. Interestingly, a previous report had demonstrated synergism between PPARγ activation and carboplatin in lung cancer cells; however, the target and exact mechanism of the increased chemosensitivity remained elusive (18, 19). Our results not only implicate MnSOD expression in the aggressiveness of the basal type breast cancers, but also provide evidence to link the anti-tumor activity of PPARγ activation to repression of this important anti-oxidant protein.

Repression of MnSOD enhances chemosensitivity via *MitoROS generation*

Since MnSOD is an important anti-oxidant protein expressed in the mitochondria, a logical explanation for these effects could

FIG. 6. Increase in MnSOD expression is associated with the development of MDA-MB-231 resistance to DOX and DOC. (A) MDA-MB-231 wild-type and Dox-resistant (DOX-R) cells were treated with 0.2, 0.4, and 1 μM of DOX for 48 h before cell number was assessed by crystal violet assay. Results shown represent mean ± SD, $n = 3$, $^*p < 0.05$ *versus* control. **(B)** MDA-MB-231 wild-type and DOC-resistant (DOC-R) cells were treated with 50, 100,, and 200 nM DOC for 48 h before cell number was assessed by crystal violet assay. Results shown represent mean ± SD, $n = 3$, $^*p < 0.05$ *versus* control. **(C)** Basal MnSOD mRNA levels in MDA-MB-231 wild-type *versus* DOX-R cells normalized to 18S mRNA levels Results are expressed as fold change against wild-type MDA-MB-231. Results shown represent mean ± SD, $n = 3$, $^*p < 0.05$ *versus* control. **(D)** Basal MnSOD protein levels in MDA-MB-231 wild-type *versus* DOX-R cells. **(E)** Basal MnSOD mRNA levels in MDA-MB-231 wild-type *versus* DOC-R cells normalized to 18S mRNA levels. Results are expressed as fold change against wild-type MDA-MB-231. Results shown represent mean ± SD, $n = 3$, $^*p < 0.05$ *versus* control. **(F)** Basal MnSOD protein levels in MDA-MB-231 wild-type *versus* MDA-MB-231 DOC-R cells. **(G)** MDA-MB-231 DOX-R cells were transfected with ctsi or 100 nM siMnSOD. Forty eight hours post transfection, cells were treated with 0.2, 0.4,, and 1 μM DOX for 48 h before cell number was assessed by crystal violet assay. Results shown represent mean ± SD, $n = 3$, $^*p < 0.05$ *versus* DOX-R ctsi untreated. **(H)** MDA-MB-231 DOC-R cells were transfected with ctsi or 100 nM siMnSOD. Forty eight hours post transfection, cells were treated with 30 and 60 nM DOC for 48 h before cell number was assessed by crystal violet assay. Results shown represent mean ± SD, $n = 3$, $^*p < 0.05$ *versus* DOC-R ctsi untreated. **(I)** MDA-MB-231 DOX-R cells were treated with 0.2, 0.4, and 1 μM DOX with and without 6 h preincubation of 10 μM 15d-PGJ_2 for 48 h before cell number was assessed by crystal violet assay. Results shown represent mean ± SD, $n = 3$, $^*p < 0.05$ *versus* DOX-R untreated. **(J)** MDA-MB-231 DOC-R cells were treated with 30 and 60 nM DOC for 48 h with and without 6 h preincubation of 10 μM 15d-PGJ_2 before cell number was assessed by crystal violet assay. Results shown represent mean ± SD, $n = 3$, $^*p < 0.05$ *versus* DOC-R untreated.

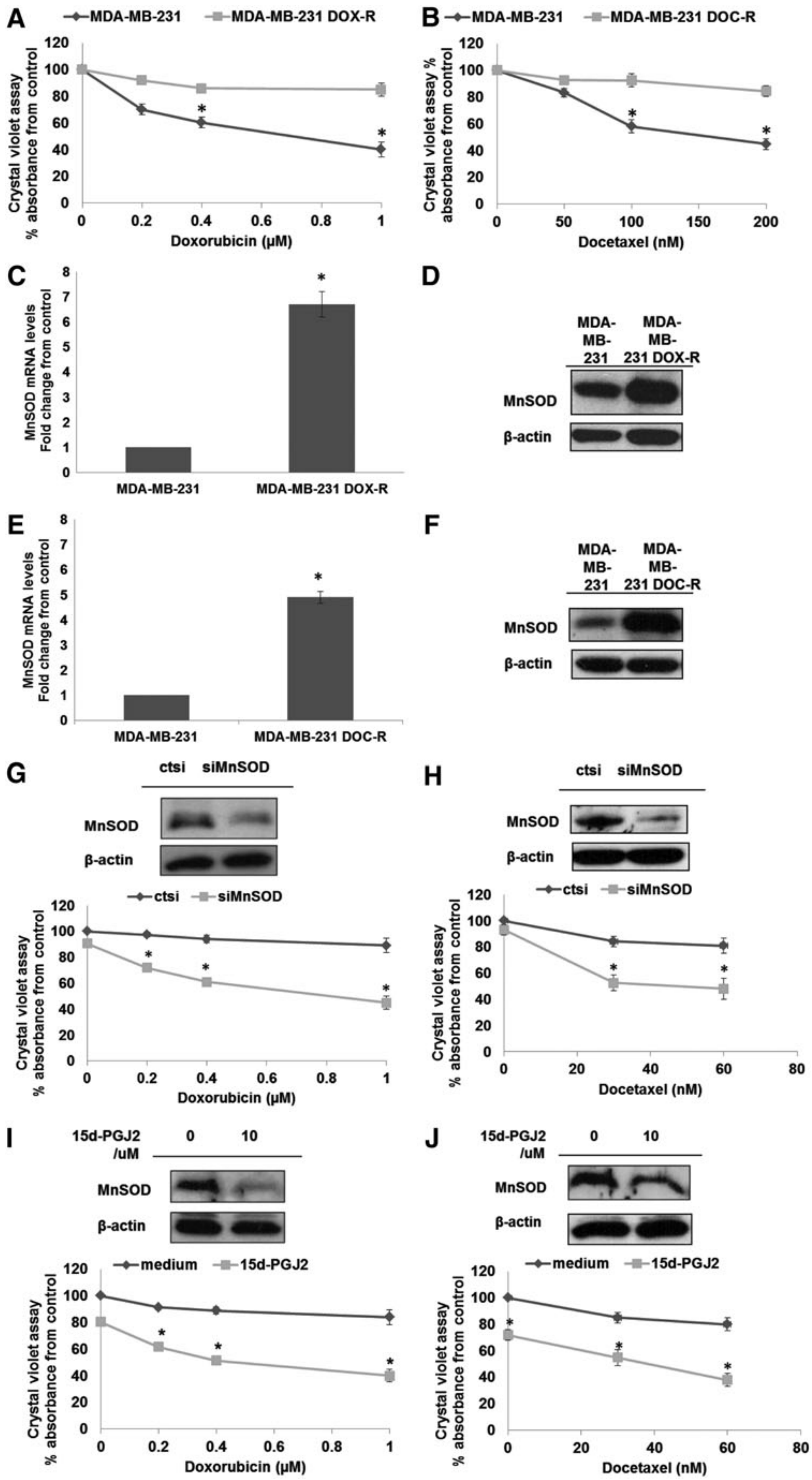
A
MDA-MB-231
MDA-MB-231 DOX-R
Crystal violet assay % absorbance from control
Doxorubicin (μM)
B
MDA-MB-231
MDA-MB-231 DOC-R
Crystal violet assay % absorbance from control
Docetaxel (nM)
C
MnSOD mRNA levels Fold change from control
MDA-MB-231
MDA-MB-231 DOX-R
D
MDA-MB-231
MDA-MB-231 DOX-R
MnSOD
β-actin
E
MnSOD mRNA levels Fold change from control
MDA-MB-231
MDA-MB-231 DOC-R
F
MDA-MB-231
MDA-MB-231 DOC-R
MnSOD
β-actin
G
ctsi
siMnSOD
MnSOD
β-actin
Crystal violet assay % absorbance from control
Doxorubicin (μM)
H
ctsi
siMnSOD
MnSOD
β-actin
Crystal violet assay % absorbance from control
Docetaxel (nM)
I
15d-PGJ2 /uM
0
10
MnSOD
β-actin
medium
15d-PGJ2
Crystal violet assay % absorbance from control
Doxorubicin (μM)
J
15d-PGJ2 /uM
0
10
MnSOD
β-actin
medium
15d-PGJ2
Crystal violet assay % absorbance from control
Docetaxel (nM)

be that an altered expression of MnSOD changes the redox milieu of cells, which could explain for the varied responses to drug treatment. Indeed, repression of MnSOD by siRNA was accompanied by an increase in mitochondrial O_2^- production in tumor cells but not in nontransformed cells. This difference could be due to the Warburg effect, as cancer cells are under intrinsic oxidative stress and require a significantly higher antioxidant capacity than their normal counterparts (53). Coupled to this is the observation that the cellular levels of a major antioxidant enzyme, glutathione peroxidase, are significantly lower in tumor cells compared with normal cells (33). Thus, the intrinsic vulnerability of tumor cells provides a window for potential therapeutic exploitation.

Interestingly, intracellular ROS have been implicated in PPARγ-induced cytotoxicity; however, it is not entirely clear whether the effect on intracellular ROS is linked to the transcriptional activity of the active nuclear receptor or a bystander effect. Our results show a clear increase in intracellular ROS as well as intra-mitochondrial O_2^- production in human breast carcinoma cell lines after exposure to the PPARγ ligands, whereas no detectable increase was observed in nontransformed cells. This could be due to the significantly lower expression of PPARγ in the nontransformed cells, thereby rendering them insensitive to low concentrations of 15d-PGJ$_2$, unlike tumor cells. This is further supported by the insignificant change in PPARγ activity when nontransformed cells were exposed to increasing doses of 15d-PGJ$_2$, thus strengthening the therapeutic potential of specifically targeting tumor cells with PPARγ ligands. It is worth pointing out that Martinez *et al.* had previously reported a similar effect of 15d-PGJ$_2$ on cellular ROS generation (46).

Based on the published reports, a number of possible mechanisms of PPARγ-induced increase in intracellular ROS have been proposed (Table 1). These reports suggest that altering redox homeostasis to activate apoptotic pathways is closely associated with PPARγ-induced cytotoxicity. We show that not only does the expression of MnSOD decrease on activation of the PPARγ receptor (by natural or synthetic ligands), but also the resultant increase in mitochondrial O_2^- could be blocked by the overexpression of MnSOD as well as by the PPARγ antagonist GW9662. Most importantly, this increase in MitoROS *via* repression of MnSOD appears to be an effector mechanism in the significant synergism observed with the combined use of PPARγ ligand and chemotherapeutic agents, DOX and DOC. The synergism is not only in terms of increased sensitivity to cell death, but also in an amplification of intracellular ROS given that DOC and DOX are known inducers of oxidative stress. A similar mechanism might explain the observed synergy between rosiglitazone and carboplatin in lung carcinoma, considering that carboplatin and other platinum-based compounds trigger an increase in MitoROS (7). Importantly, the involvement of the reactive $ONOO^-$ *via* the reaction between mitochondria-dependent O_2^- and NO production is proposed. This observation is further supported by the use of ROS scavengers Tiron and FeTPPS, which effectively attenuated the chemosensitization caused by PPARγ-induced repression or gene knockdown of MnSOD in the basal breast carcinoma. Similar findings implicating $ONOO^-$ as an effector molecule in inducing cancer cell cytotoxicity have recently been reported (16, 66, 71). These independent reports provide precedence to the possible involvement of $ONOO^-$ in the enhanced chemosensitivity of basal breast carcinoma on targeting MnSOD expression by PPARγ ligands.

Therefore, these results support the correlation between MnSOD repression by PPARγ activation, and increased oxidative stress in tumor cells. It also provides an explanation for other studies that associated MnSOD deficiencies to an increase in intracellular ROS production (45, 67, 70).

FIG. 7. Down-regulation of MnSOD expression by siMnSOD or activation of PPARγ induces an increase in Mitochondrial reactive oxygen species (MitoROS) in tumor cells. (A) MDA-MB-231 were transfected with ctsi or 100 n*M* MnSOD small-interfering RNA (siRNA). Post transfection, cells were incubated with and without 10 m*M* N-acetyl cysteine (NAC) for 48 h. *Top panel*: Western blot analysis of MnSOD protein levels. *Bottom panel*: Mitochondrial superoxide ($O_2^{\bullet-}$) production was measured using MitoSOX Red assay. Results are expressed as percentage increases in arbitrary units (a.u.) relative to ctsi. Results shown represent mean ± SD, $n=3$, *$p<0.05$ *versus* ctsi. **(B)** Mitochondrial $O_2^{\bullet-}$ was measured in MDA-MB-231 with and without preincubation of 10 m*M* NAC for 4 h followed by 10 μM 15d-PGJ$_2$ treatment for 16 h using MitoSOX Red assay. Results are expressed as percentage increases in a.u. from control. Results shown represent mean ± SD, $n=3$, *$p<0.05$ *versus* control. **(C)** MDA-MB-231 cells were transfected with 2 μg human MnSOD plasmid or empty vector pcDNA3. Forty eight hours post transfection, cells were treated with 10 μM 15d-PGJ$_2$ treatment for 16 h. *Top panel*: Western blot analysis of MnSOD protein levels after transfection followed by 15d-PGJ$_2$ treatment. *Bottom panel*: Mitochondrial $O_2^{\bullet-}$ production was measured using MitoSOX Red assay. Results are expressed as percentage increases in a.u. relative to pcDNA3. Results shown represent mean ± SD, $n=3$, *$p<0.05$ *versus* pcDNA3. **(D)** *Top panel*: Western blot of MDA-MB-231 cells transfected with empty vector pcDNA3 or 2 μg MnSOD plasmid. Forty eight hours post transfection, cells were treated with 80 μM rosiglitazone for 24 h. *Bottom panel*: Mitochondrial $O_2^{\bullet-}$ production was measured using MitoSOX Red assay. Results shown represent mean ± SD, $n=3$, *$p<0.05$ *versus* control. **(E)** *Top panel*: Western blot of MDA-MB-231 cells transfected with empty vector pcDNA3 or 2 μg MnSOD plasmid. Forty eight hours post transfection, cells were treated with 50 μM troglitazone for 24 h. *Bottom panel*: Mitochondrial $O_2^{\bullet-}$ production was measured using MitoSOX Red assay. Results shown represent mean ± SD, $n=3$, *$p<0.05$ *versus* control. **(F)** Mitochondrial $O_2^{\bullet-}$ production in MDA-MB-231 on 10 μM 15d-PGJ$_2$ treatment with and without 4 h preincubation with 10 μM GW9662 was measured using MitoSOX Red assay. Results are expressed as percentage increases in a.u. from control. Results shown represent mean ± SD, $n=3$, *$p<0.05$ *versus* control. **(G)** Mitochondrial $O_2^{\bullet-}$ production in MDA-MB-231 on 40 and 80 μM rosiglitazone treatment with and without 4 h preincubation with 10 μM GW9662 was measured using MitoSOX Red assay. Results are expressed as percentage increases in a.u. relative to control. Results shown represent mean ± SD, $n=3$, *$p<0.05$ *versus* control. **(H)** Mitochondrial $O_2^{\bullet-}$ production in MDA-MB-231 on 20 and 50 μM troglitazone treatment with and without 4 h preincubation with 10 μM GW9662 was measured using MitoSOX Red assay. Results are expressed as percentage increases in a.u. relative to control. Results shown represent mean ± SD, $n=3$, *$p<0.05$ *versus* control.

Concluding remarks

In conclusion, our study not only highlights the association between increased MnSOD expression and an aggressive subtype of breast cancer, but also provides evidence for the judicious use of PPARγ agonists as chemosensitizers in this particular subtype of breast cancer for targeted ROS-mediated strategy that warrants serious consideration in the clinical settings.

Materials and Methods

Reagents

Roswell Park Memorial Institute (RPMI) 1640 medium, Dulbecco's modified Eagle's medium, phosphate-buffered saline (PBS), fetal bovine serum (FBS), charcoal-stripped FBS, L-glutamine, and trypsin were purchased from Hyclone. Pepstatin

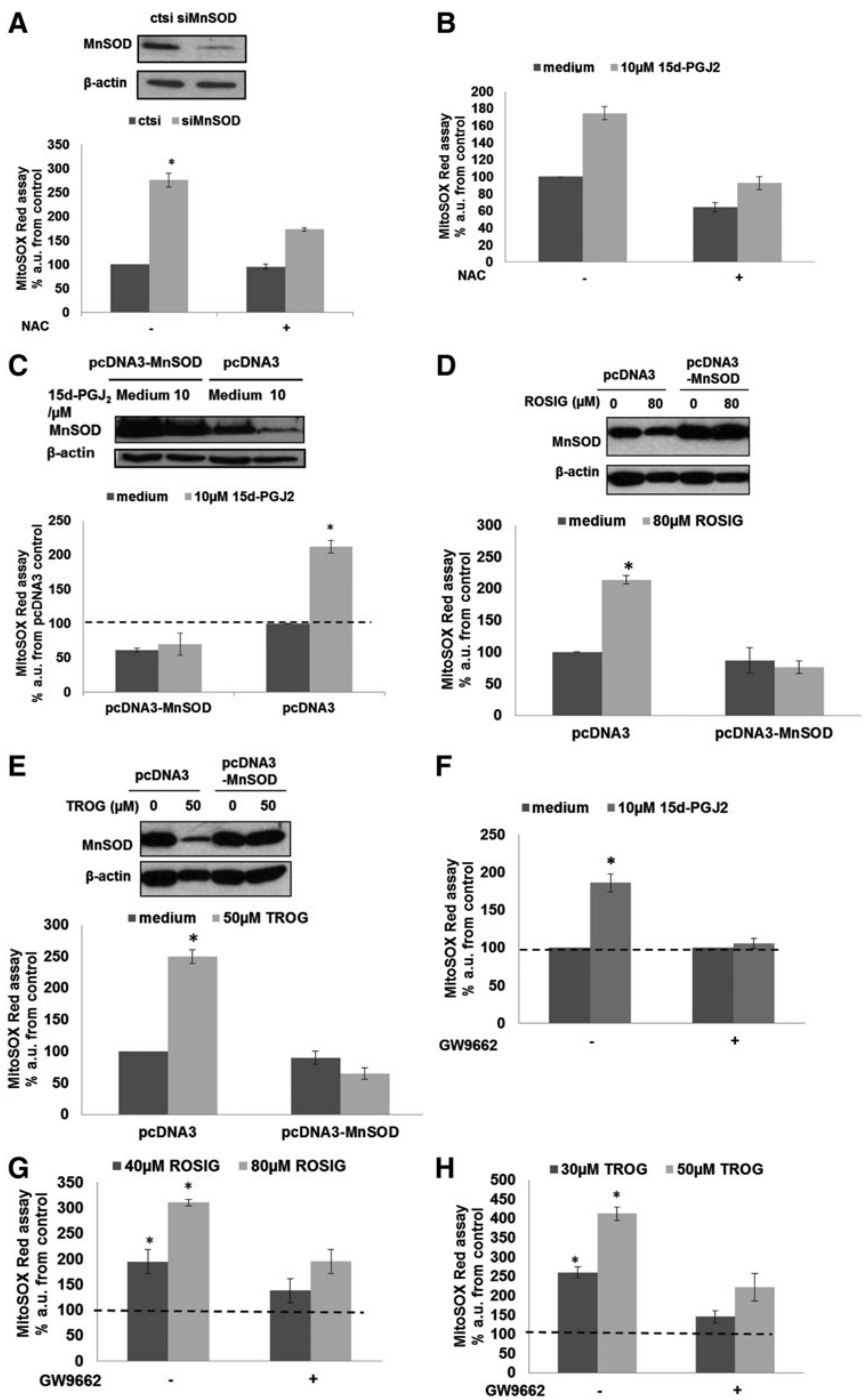

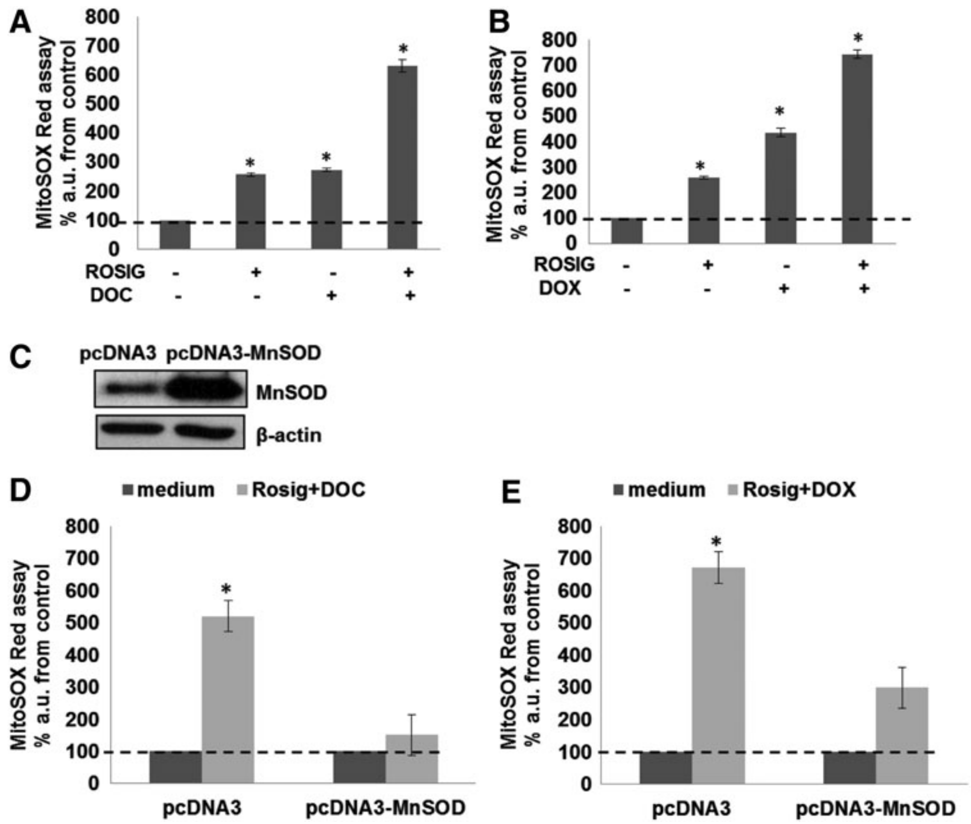

FIG. 8. Chemosensitization of MDA-MB-231 cells is dependent on down-regulation of MnSOD by PPARγ activation. **(A)** MDA-MB-231 cells were treated with 80 μM rosiglitazone alone, 60 nM DOC alone, or in combination for 24 h. Mitochondrial $O_2^{\bullet -}$ production was measured using MitoSOX Red assay. **(B)** MDA-MB-231 cells were treated with 80 μM rosiglitazone alone, 0.4 μM DOX alone, or in combination for 24 h. Mitochondrial $O_2^{\bullet -}$ production was measured using MitoSOX Red assay. Results shown represent mean ± SD, $n = 3$, *$p < 0.05$ *versus* control. **(C)** Western blot of MDA-MB-231 cells transfected with empty vector pcDNA3 or 2 μg MnSOD plasmid. **(D)** Forty eight hours post transfection, cells from **(C)** were treated with 80 μM rosiglitazone and 60 nM DOC in combination for 24 h before mitochondrial $O_2^{\bullet -}$ production was measured using MitoSOX Red assay. **(E)** Forty eight hours post transfection, cells from **(C)** were treated with 80 μM rosiglitazone and 0.4 μM DOX in combination for 24 h before mitochondrial $O_2^{\bullet -}$ production was measured using MitoSOX Red assay. Results shown represent mean ± SD, $n = 3$, *$p < 0.05$ *versus* control.

A, phenylmethanesulfonyl fluoride (PMSF), leupeptin, propidium iodide, crystal violet, 3-(4,5-Dimethylthiazol-2-yl)-2,5-diphenyltetrazolium bromide (MTT), bovine serum albumin, mouse anti-β-actin monoclonal antibody, DOC, DOX, catalase, and tiron were supplied by Sigma-Aldrich. Aprotinin was purchased from Applichem. Rabbit anti-HuMnSOD monoclonal antibody was purchased from Upstate. Mouse anti-HuPPARγ and anti-Huβ-actin monoclonal antibodies were purchased from Santa Cruz Biotechnology. Stabilized goat anti-mouse horseradish peroxidase (HRP) and goat anti-rabbit HRP were

FIG. 9. Chemosensitization of MDA-MB-231 cells on down-regulation of MnSOD expression involves nitric oxide (NO) production. **(A)** MDA-MB-231 were transfected with 100 nM ctsi and siMnSOD. NO production was measured using DAF assay. Results are expressed as percentage increase in a.u. relative to ctsi. Results shown represent mean ± SD, $n = 3$, *$p < 0.05$ *versus* ctsi. **(B)** MDA-MB-231 cells were treated with 80 μM rosiglitazone alone, 60 nM DOC alone, or in combination for 24 h. NO production was measured using DAF assay. **(C)** MDA-MB-231 cells were treated with 80 μM rosiglitazone alone, 0.4 μM DOX alone, or in combination for 24 h. NO production was measured using DAF assay. Results shown represent mean ± SD, $n = 3$, *$p < 0.05$ *versus* control. **(D)** MDA-MB-231 cells with and without preincubation of 10 mM NAC for 4 h were treated with 80 μM rosiglitazone, 60 nM DOC, or both for 24 h before mitochondrial $O_2^{\bullet -}$ production was measured by MitoSOX Red assay. **(E)** MDA-MB-231 cells with and without preincubation of 10 mM NAC for 4 h were treated with 80 μM rosiglitazone, 0.4 μM DOX, or both for 24 h before mitochondrial $O_2^{\bullet -}$ production was measured by MitoSOX Red assay. **(F)** MDA-MB-231 cells with and without preincubation of 10 mM Tiron for 4 h were treated with 80 μM rosiglitazone, 60 nM DOC, or both for 24 h before mitochondrial $O_2^{\bullet -}$ production was measured by MitoSOX Red assay. **(G)** MDA-MB-231 cells with and without preincubation of 10 mM Tiron for 4 h were treated with 80 μM rosiglitazone, 0.4 μM DOX, or both for 24 h before mitochondrial $O_2^{\bullet -}$ production was measured by MitoSOX Red assay. **(H)** MDA-MB-231 cells with and without preincubation of 3000 U/ml catalase for 4 h were treated with 80 μM rosiglitazone, 60 nM DOC, or both for 24 h before mitochondrial $O_2^{\bullet -}$ production was measured by MitoSOX Red assay. **(I)** MDA-MB-231 cells with and without preincubation of 3000 U/ml catalase for 4 h were treated with 80 μM rosiglitazone, 0.4 μM DOX, or both for 24 h before mitochondrial $O_2^{\bullet -}$ production was measured by MitoSOX Red assay. Results shown represent mean ± SD, $n = 3$, *$p < 0.05$ *versus* control.

obtained from Pierce. Methanol and sodium dodecyl sulfate were purchased from Merck. Cell lysis buffer (1×) was from BD Pharmigen. The PPARγ agonist, 15d-PGJ_2 was purchased from Alexis Biochemical. MitoSOX Red and DAF-FM reagents were purchased from Molecular Probes, Invitrogen.

Cell lines and culture conditions

ER-negative MDA-MB-231, MDA-MB-468, BT-549, MCF-10A, and 184A1 breast cancer cells (American Type Culture Collection) were used. Cells lines were routinely maintained

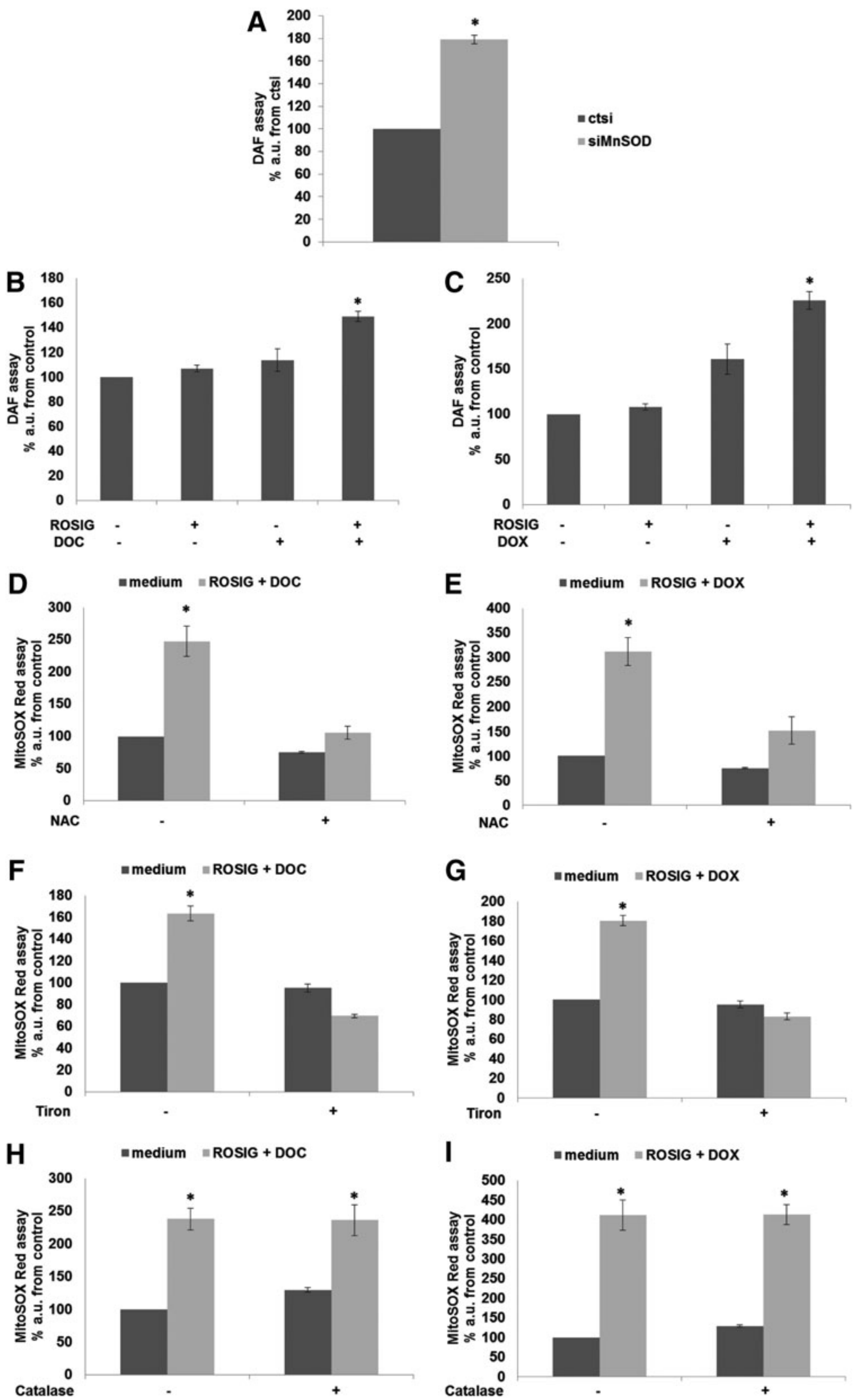

in RPMI 1640 for tumor cell lines and mammary epithelial cell growth medium for normal epithelial cell lines supplemented with 10% FBS, 2 m*M* L-glutamine and 0.05 mg/ml gentamicin (Cambrex Bio Science Walkersville, Inc.) in a 37°C incubator with 5% CO_2.

Western blot analysis

Western blot was performed as previously described (1). For details, refer to Supplementary data.

RNA isolation, reverse transcription, and real-time polymerase chain reaction

Total RNA was isolated from cells by TRIZOL reagent (Invitrogen), as described by the manufacturer's instructions. Reverse-transcription reaction was carried out using ABI PRISM 7500 (Applied Biosystems). Primers and probe for human 18S, human PPARγ, and human MnSOD were purchased from Applied Biosystems (Assays on Demand). For details, refer to Supplementary data.

Transfection

In vitro transfections were done using LipofectAMINE 2000 (Invitrogen) following the manufacturer's protocols. For silencing studies, 200 n*M* of MnSOD siRNA (5′-AAAUUGCU GCUUGUCCAAAUC-3′) (17) or scrambled control siRNA (5′-AGCUUCAUAAGGCGCAUGCTT-3′ [luciferase gene sequence inverted]) was transiently transfected into MDA-MB-231 and 184A1 using LipofectAMINE RNAiMAX (Invitrogen) following the manufacturer's protocols.

MTT assay

Cell number after drug treatment was assessed by MTT assay as previously described (44).

Crystal violet assay

Cell number after drug treatment was assessed by crystal violet uptake assay as previously described (1).

MitoSOX red assay

Intracellular mitochondrial O_2^- production was detected *via* MitoSOX Red (Invitrogen) staining as previously described (44).

DAF assay

Intracellular NO production was detected *via* DAF-FM (Invitrogen) staining as per manufacturer's instructions.

Luciferase assay

The luciferase reporter construct used was pPPRE-tk-Luc, which contains three PPREs from rat acyl-CoA oxidase promoter under the control of the Herpes simplex virus thymidine kinase promoter. PPRE promoter activities were assessed with a dual-luciferase assay kit. Bioluminescence generated was measured using a Sirius luminometer (Berthold). The luminescence readings obtained were normalized to the protein content of the corresponding cell lysate.

Colony forming assay

Cells transfected with control scrambled siRNA (ctsi) and siMnSOD were subjected to DOC and DOX treatment for 48 h. After this, cells were trysinised and 15,000 cells per treatment were re-seeded into 100 mm dishes and left to grow for 10 to 15 days with complete medium. At the end of the assay, cells were washed and stained with crystal violet.

Soft agar colony forming assay

Soft agar colony formation assay was performed in 96-well plates after MnSOD siRNA transfection followed by DOC and DOX treatment. Briefly, 5×10^3 cells were seeded into 100 ml 0.35% agarose onto the 0.5% agarose base layer. Serum supplemented medium (100 ml) containing drug was added on the top and changed every 3 days. After 10 days, total number of colonies per well that were >100 microns in size when viewed under a simple microscope were counted (31). Light microscopy images were captured under 100× magnification.

Mouse xenograft model

To determine the *in vivo* activity of 15d-PGJ_2, viable MDA-MB-231 cells (1×10^7) resuspended in 100 μl Matrigel and PBS were injected into the mammary fat pad of 6-week-old female Balb/c nude mice (Orient Bio, Inc.). When average subcutaneous tumor volume reached 50–70 mm^3, mice were assigned into two treatment groups: (i) control

FIG. 10. Chemosensitization of MDA-MB-231 cells on down-regulation of MnSOD expression is mediated by $ONOO^-$. (A) MDA-MB-231 cells with and without preincubation of 10 m*M* NAC for 4 h were treated with 80 μM rosiglitazone, 60 n*M* DOC, or both for 48 h before cell viability was assessed by crystal violet assay. **(B)** MDA-MB-231 cells with and without preincubation of 10 m*M* NAC for 4 h were treated with 80 μM rosiglitazone, 0.4 μM DOX, or both for 48 h before cell viability was assessed by crystal violet assay. **(C)** MDA-MB-231 cells with and without preincubation of 10 m*M* Tiron for 4 h were treated with 80 μM rosiglitazone, 60 n*M* DOC, or both for 48 h before cell viability was assessed by crystal violet assay. **(D)** MDA-MB-231 cells with and without preincubation of 10 m*M* Tiron for 4 h were treated with 80 μM rosiglitazone, 0.4 μM DOX, or both for 48 h before cell viability was assessed by crystal violet assay. **(E)** MDA-MB-231 cells with and without preincubation of 100 μM 5,10,15,20-Tetrakis(4-sulfonatophenyl)porphyrinato Iron (III), Chloride (FeTPPS) for 4 h were treated with 80 μM rosiglitazone, 60 nM DOC, or both for 48 h before cell viability was assessed by crystal violet assay. **(F)** MDA-MB-231 cells with and without preincubation of 100 μM FeTPPS for 4 h were treated with 80 μM rosiglitazone, 0.4 μM DOX, or both for 48 h before cell viability was assessed by crystal violet assay. **(G)** MDA-MB-231 cells with and without preincubation of 3000 U/ml catalase for 4 h were treated with 80 μM rosiglitazone, 60 nM DOC, or both for 48 h before cell viability was assessed by crystal violet assay. **(H)** MDA-MB-231 cells with and without preincubation of 3000 U/ml catalase for 4 h were treated with 80 μM rosiglitazone, 0.4 μM DOX, or both for 48 h before cell viability was assessed by crystal violet assay. Results shown represent mean ± SD, $n=3$, *$p<0.05$ *versus* control. **(I)** Proposed model for chemosensitization of basal-like breast carcinoma upon inhibition of MnSOD expression.

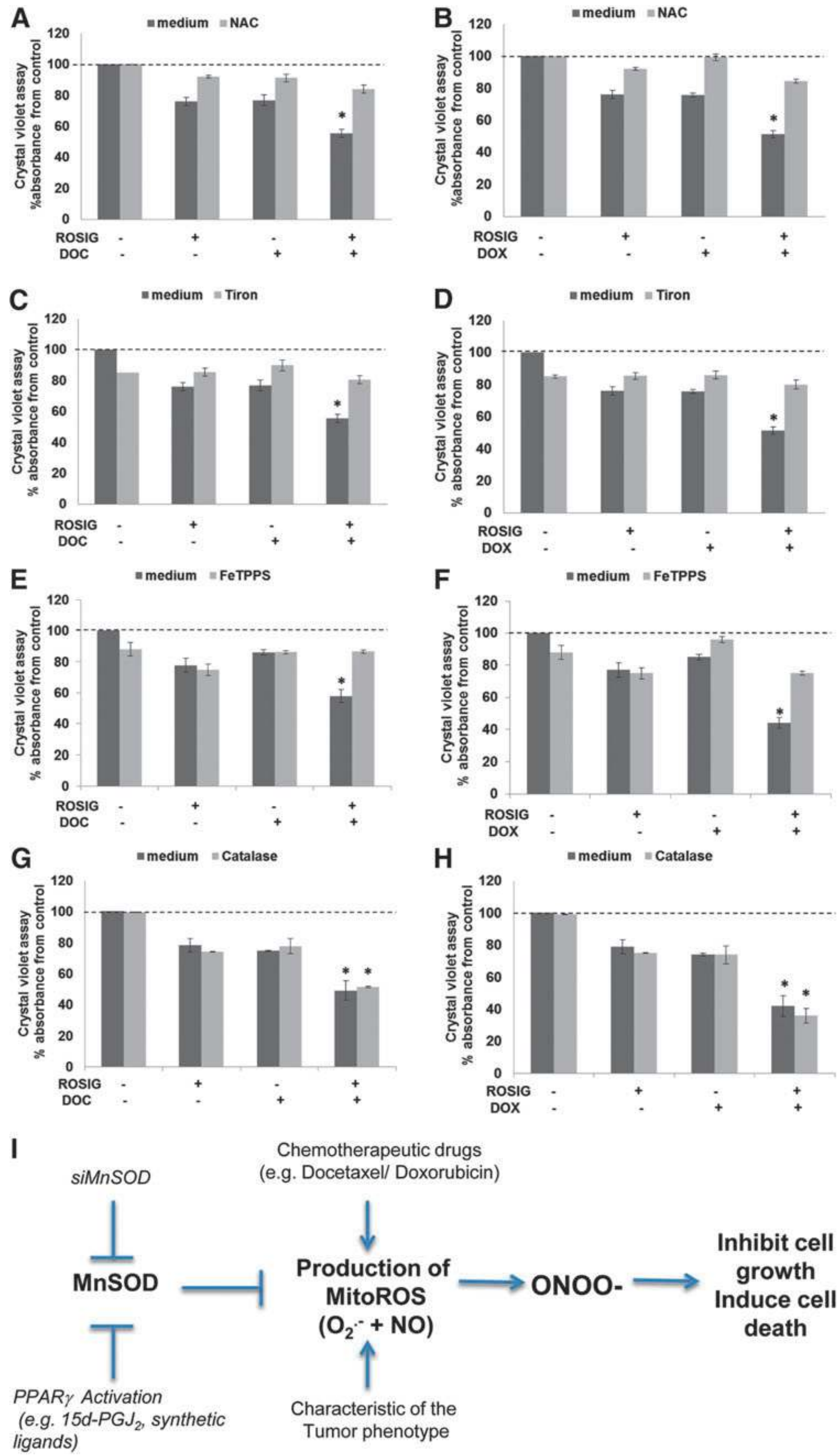
A
medium NAC
Crystal violet assay %absorbance from control
ROSIG
DOC
B
medium NAC
Crystal violet assay %absorbance from control
ROSIG
DOX
C
medium Tiron
Crystal violet assay % absorbance from control
ROSIG
DOC
D
medium Tiron
Crystal violet assay % absorbance from control
ROSIG
DOX
E
medium FeTPPS
Crystal violet assay % absorbance from control
ROSIG
DOC
F
medium FeTPPS
Crystal violet assay % absorbance from control
ROSIG
DOX
G
medium Catalase
Crystal violet assay % absorbance from control
ROSIG
DOC
H
medium Catalase
Crystal violet assay % absorbance from control
ROSIG
DOX
I
siMnSOD
Chemotherapeutic drugs
(e.g. Docetaxel/ Doxorubicin)
MnSOD
Production of MitoROS ($O_2^{\cdot -}$ + NO)
ONOO-
Inhibit cell growth Induce cell death
PPARγ Activation
(e.g. 15d-PGJ$_2$, synthetic ligands)
Characteristic of the Tumor phenotype

(vehicle only) and (ii) 15d-PGJ_2 given at a dose of 5 mg/kg *via* tail vein every 3 days. Control groups were treated with vehicle. Tumor size was measured daily with a caliper (calculated volume = shortest diameter^2 × longest diameter/2). Mice were followed for tumor size and body weight and were sacrificed on the 18th day. Tumors were resected, weighed, and frozen or fixed in formalin and paraffin embedded for IHC studies.

Clinicopathological data

The study material comprised 15 cases of mammary carcinoma diagnosed at or referred to National University Hospital, Singapore, between 2004 and 2006 (37).

Immunohistochemistry for MnSOD

IHC detection of MnSOD antigen was done on formalin-fixed, paraffin-embedded tumor breast tissues. Stained sections were viewed on an Arcturus PixCell II LCM System. Pictures of stained sections were taken using an Olympus camera (Model C5050). The expression status of MnSOD was scored by following standard 4-tiered scoring practice, ranging from 0 to +3. For statistical analyses, negative (0) and weak expression (+1) were grouped together and termed 'low expression' of the proteins. Moderate (+2) and strong (+3) expression was termed 'high expression'.

Generation of DOX- and DOC-resistant cells

Generation of MDA-MB-231 DOX- and DOC-resistant cells was carried out by exposing cells first to one-tenth of IC50 for 24 h before replacing with fresh medium. Cells were then allowed to proliferate before exposure to stepwise increasing concentrations of the drug for 24 h each time. The starting dose of DOX used was 0.1 μM, and the dose was increased by 0.1 μM each time. The starting dose of DOC used was 10 nM, and the dose was increased by 10 nM each time. Cells were passaged whenever 80%–90% confluency was reached. After 4–6 weeks, cell viability assay was carried out on parental (drug sensitive) and drug-resistant cell lines to measure fold resistance.

Data preprocessing of TCGA and affymetrix breast cancer data

Invasive ductal breast cancer data were downloaded from TCGA (http://cancergenome.nih.gov/). For this study, we included all 536 available breast tumor gene expression data at the time that the analysis was initiated in October 2011. The data are on Agilent custom gene expression microarray G4502A_07. The data were imported to Partek® Genomics Suite 6.6, where the log ratio of gene expression value was quantile normalized for further analysis.

Breast cancer data on Affymetrix U133A or U133Plus2 platforms were downloaded from Array Express and GEO. The panel of human breast cancer data utilized for analysis comprises 3992 tumor samples from 26 cohorts (22). Robust Multichip Average normalization was performed on each dataset. The normalized data were combined and subsequently standardized using ComBat (29) to remove batch effect.

Identification of breast cancer subtypes

Breast cancer subtype signature was obtained from Prat *et al.*, 2010 (57). Subsequently, ssGSEA (65) was computed based on the breast cancer subtype signature for each sample. Each sample was then assigned to be the subtype under which it has the maximum ssGSEA score.

Statistical analysis

Statistical analysis was performed using paired Student's *t*-test. A *p*-value of < 0.05 was considered significant. Statistical significance evaluation by Mann–Whitney test and Spearman correlation test were computed using Matlab®. Dot plot and Kaplan–Meier analysis were done using Graphpad Prism.

Acknowledgments

PPARγ mutant (PPARγC126A/E127A) (PPARγDN) (25) was kindly provided by Christopher K. Glass (UCSD, San Diego, CA). The pcDNA3-MnSOD plasmid was kindly provided by Daret St. Clair (University of Kentucky College of Medicine, Lexington, KY). The luciferase reporter construct pPPRE-tk-Luc was a kind gift from Ronald M. Evans, The Salk Institute for Biological Studies, San Diego, CA.

This work was supported by grants from the National Medical Research Council, Singapore, to M.V.C., S.P., and A.P.K. [R-183-000-204-213] and to A.P.K., M.V.C., and S.P. [R-713-000-124-213]. A.P.K. and S.P. are also supported by the Cancer Science Institute of Singapore, Experimental Therapeutics I Program [Grant R-713-001-011-271]. J.I.P. was supported by the Korea Science and Engineering Foundation (KOSEF) grant funded by the Korean government (MEST) [R13-2002-044-05002-0].

Author Disclosure Statement

No competing financial interests exist.

References

1. Akram S, Teong HF, Fliegel L, Pervaiz S, and Clement MV. Reactive oxygen species-mediated regulation of the Na+-H+ exchanger 1 gene expression connects intracellular redox status with cells' sensitivity to death triggers. *Cell Death Differ* 13: 628–641, 2006.
2. Altenberg B and Greulich KO. Genes of glycolysis are ubiquitously overexpressed in 24 cancer classes. *Genomics* 84: 1014–1020, 2004.
3. Alvarez-Maqueda M, El Bekay R, Alba G, Monteseirin J, Chacon P, Vega A, Martin-Nieto J, Bedoya FJ, Pintado E, and Sobrino F. 15-deoxy-delta 12,14-prostaglandin J2 induces heme oxygenase-1 gene expression in a reactive oxygen species-dependent manner in human lymphocytes. *J Biol Chem* 279: 21929–21937, 2004.
4. Bravard A, Sabatier L, Hoffschir F, Ricoul M, Luccioni C, and Dutrillaux B. SOD2: a new type of tumor-suppressor gene? *Int J Cancer* 51: 476–480, 1992.
5. Chen PM, Wu YH, Li MC, Cheng YW, Chen CY, and Lee H. MnSOD promotes tumor invasion via upregulation of FoxM1-MMP2 axis and related with poor survival and relapse in lung adenocarcinomas. *Mol Cancer Res* 11: 261–271, 2012.
6. Chen YC, Shen SC, and Tsai SH. Prostaglandin D(2) and J(2) induce apoptosis in human leukemia cells via activation of

the caspase 3 cascade and production of reactive oxygen species. *Biochim Biophys Acta* 1743: 291–304, 2005.
7. Cheng CF, Juan SH, Chen JJ, Chao YC, Chen HH, Lian WS, Lu CY, Chang CI, Chiu TH, and Lin H. Pravastatin attenuates carboplatin-induced cardiotoxicity via inhibition of oxidative stress associated apoptosis. *Apoptosis* 13: 883–894, 2008.
8. Clement MV and Pervaiz S. Intracellular superoxide and hydrogen peroxide concentrations: a critical balance that determines survival or death. *Redox Rep* 6: 211–214, 2001.
9. Cobbs CS, Levi DS, Aldape K, and Israel MA. Manganese superoxide dismutase expression in human central nervous system tumors. *Cancer Res* 56: 3192–3195, 1996.
10. Dhar SK and St Clair DK. Manganese superoxide dismutase regulation and cancer. *Free Radic Biol Med* 52: 2209–2222, 2012.
11. Dhar SK, Tangpong J, Chaiswing L, Oberley TD, and St Clair DK. Manganese superoxide dismutase is a p53-regulated gene that switches cancers between early and advanced stages. *Cancer Res* 71: 6684–6695, 2011.
12. DuBois RN, Gupta R, Brockman J, Reddy BS, Krakow SL, and Lazar MA. The nuclear eicosanoid receptor, PPAR-gamma, is aberrantly expressed in colonic cancers. *Carcinogenesis* 19: 49–53, 1998.
13. Echiburu-Chau C, Roy D, and Calaf GM. Metastatic suppressor CD44 is related with oxidative stress in breast cancer cell lines. *Int J Oncol* 39: 1481–1489, 2011.
14. Elstner E, Muller C, Koshizuka K, Williamson EA, Park D, Asou H, Shintaku P, Said JW, Heber D, and Koeffler HP. Ligands for peroxisome proliferator-activated receptorgamma and retinoic acid receptor inhibit growth and induce apoptosis of human breast cancer cells *in vitro* and in BNX mice. *Proc Natl Acad Sci U S A* 95: 8806–8811, 1998.
15. Ennen M, Minig V, Grandemange S, Touche N, Merlin JL, Besancenot V, Brunner E, Domenjoud L, and Becuwe P. Regulation of the high basal expression of the manganese superoxide dismutase gene in aggressive breast cancer cells. *Free Radic Biol Med* 50: 1771–1779, 2011.
16. Fraszczak J, Trad M, Janikashvili N, Cathelin D, Lakomy D, Granci V, Morizot A, Audia S, Micheau O, Lagrost L, Katsanis E, Solary E, Larmonier N, and Bonnotte B. Peroxynitrite-dependent killing of cancer cells and presentation of released tumor antigens by activated dendritic cells. *J Immunol* 184: 1876–1884, 2010.
17. Funasaka T, Hu H, Hogan V, and Raz A. Down-regulation of phosphoglucose isomerase/autocrine motility factor expression sensitizes human fibrosarcoma cells to oxidative stress leading to cellular senescence. *J Biol Chem* 282: 36362–36369, 2007.
18. Girnun GD, Chen L, Silvaggi J, Drapkin R, Chirieac LR, Padera RF, Upadhyay R, Vafai SB, Weissleder R, Mahmood U, Naseri E, Buckley S, Li D, Force J, McNamara K, Demetri G, Spiegelman BM, and Wong KK. Regression of drug-resistant lung cancer by the combination of rosiglitazone and carboplatin. *Clin Cancer Res* 14: 6478–6486, 2008.
19. Girnun GD, Naseri E, Vafai SB, Qu L, Szwaya JD, Bronson R, Alberta JA, and Spiegelman BM. Synergy between PPAR-gamma ligands and platinum-based drugs in cancer. *Cancer Cell* 11: 395–406, 2007.
20. Giulivi C, Poderoso JJ, and Boveris A. Production of nitric oxide by mitochondria. *J Biol Chem* 273: 11038–11043, 1998.
21. Greenlee RT, Hill-Harmon MB, Murray T, and Thun M. Cancer statistics, 2001. *CA Cancer J Clin* 51: 15–36, 2001.
22. Hess KR, Anderson K, Symmans WF, Valero V, Ibrahim N, Mejia JA, Booser D, Theriault RL, Buzdar AU, Dempsey PJ, Rouzier R, Sneige N, Ross JS, Vidaurre T, Gomez HL, Hortobagyi GN, and Pusztai L. Pharmacogenomic predictor of sensitivity to preoperative chemotherapy with paclitaxel and fluorouracil, doxorubicin, and cyclophosphamide in breast cancer. *J Clin Oncol* 24: 4236–4244, 2006.
23. Hileman EO, Liu J, Albitar M, Keating MJ, and Huang P. Intrinsic oxidative stress in cancer cells: a biochemical basis for therapeutic selectivity. *Cancer Chemother Pharmacol* 53: 209–219, 2004.
24. Houseknecht KL, Cole BM, and Steele PJ. Peroxisome proliferator-activated receptor gamma (PPARgamma) and its ligands: a review. *Domest Anim Endocrinol* 22: 1–23, 2002.
25. Huang Y, He T, and Domann FE. Decreased expression of manganese superoxide dismutase in transformed cells is associated with increased cytosine methylation of the SOD2 gene. *DNA Cell Biol* 18: 643–652, 1999.
26. Hur GC, Cho SJ, Kim CH, Kim MK, Bae SI, Nam SY, Park JW, Kim WH, and Lee BL. Manganese superoxide dismutase expression correlates with chemosensitivity in human gastric cancer cell lines. *Clin Cancer Res* 9: 5768–5775, 2003.
27. Izutani R, Asano S, Imano M, Kuroda D, Kato M, and Ohyanagi H. Expression of manganese superoxide dismutase in esophageal and gastric cancers. *J Gastroenterol* 33: 816–822, 1998.
28. Janssen A, Bosman C, van Duijn W, Oostendorp-van de Ruit M, Kubben F, Griffioen G, Lamers C, van Krieken J, van de Velde C, and Verspaget H. Superoxide dismutases in gastric and esophageal cancer and the prognostic impact in gastric cancer. *Clin Cancer Res* 6: 3183–3192, 2000.
29. Johnson WE, Li C, and Rabinovic A. Adjusting batch effects in microarray expression data using empirical Bayes methods. *Biostatistics* 8: 118–127, 2007.
30. Kang DW, Choi CH, Park JY, Kang SK, and Kim YK. Ciglitazone induces caspase-independent apoptosis through down-regulation of XIAP and survivin in human glioma cells. *Neurochem Res* 33: 551–561, 2008.
31. Kang J, Perry JK, Pandey V, Fielder GC, Mei B, Qian PX, Wu ZS, Zhu T, Liu DX, and Lobie PE. Artemin is oncogenic for human mammary carcinoma cells. *Oncogene* 28: 2034–2045, 2009.
32. Kao J, Salari K, Bocanegra M, Choi YL, Girard L, Gandhi J, Kwei KA, Hernandez-Boussard T, Wang P, Gazdar AF, Minna JD, and Pollack JR. Molecular profiling of breast cancer cell lines defines relevant tumor models and provides a resource for cancer gene discovery. *PLoS One* 4: e6146, 2009.
33. Kattan Z, Minig V, Leroy P, Dauca M, and Becuwe P. Role of manganese superoxide dismutase on growth and invasive properties of human estrogen-independent breast cancer cells. *Breast Cancer Res Treat* 108: 203–215, 2008.
34. Kim JJ, Chae SW, Hur GC, Cho SJ, Kim MK, Choi J, Nam SY, Kim WH, Yang HK, and Lee BL. Manganese superoxide dismutase expression correlates with a poor prognosis in gastric cancer. *Pathobiology* 70: 353–360, 2002.
35. Koppenol WH, Bounds PL, and Dang CV. Otto Warburg's contributions to current concepts of cancer metabolism. *Nat Rev Cancer* 11: 325–337, 2011.
36. Kubota T, Koshizuka K, Williamson EA, Asou H, Said JW, Holden S, Miyoshi I, and Koeffler HP. Ligand for peroxisome proliferator-activated receptor gamma (troglitazone) has potent antitumor effect against human prostate cancer both *in vitro* and *in vivo*. *Cancer Res* 58: 3344–3352, 1998.

37. Kumar AP, Quake AL, Chang MK, Zhou T, Lim KS, Singh R, Hewitt RE, Salto-Tellez M, Pervaiz S, and Clement MV. Repression of NHE1 expression by PPARgamma activation is a potential new approach for specific inhibition of the growth of tumor cells *in vitro* and *in vivo*. *Cancer Res* 69: 8636–8644, 2009.
38. Kwon CH, Park JY, Kim TH, Woo JS, and Kim YK. Ciglitazone induces apoptosis via activation of p38 MAPK and AIF nuclear translocation mediated by reactive oxygen species and Ca(2+) in opossum kidney cells. *Toxicology* 257: 1–9, 2009.
39. Landriscina M, Remiddi F, Ria F, Palazzotti B, De Leo ME, Iacoangeli M, Rosselli R, Scerrati M, and Galeotti T. The level of MnSOD is directly correlated with grade of brain tumours of neuroepithelial origin. *Br J Cancer* 74: 1877–1885, 1996.
40. Lapillonne H, Konopleva M, Tsao T, Gold D, McQueen T, Sutherland RL, Madden T, and Andreeff M. Activation of peroxisome proliferator-activated receptor gamma by a novel synthetic triterpenoid 2-cyano-3,12-dioxooleana-1,9-dien-28-oic acid induces growth arrest and apoptosis in breast cancer cells. *Cancer Res* 63: 5926–5939, 2003.
41. Lee SJ, Kim MS, Park JY, Woo JS, and Kim YK. 15-Deoxy-delta 12,14-prostaglandin J2 induces apoptosis via JNK-mediated mitochondrial pathway in osteoblastic cells. *Toxicology* 248: 121–129, 2008.
42. Levine AJ and Puzio-Kuter AM. The control of the metabolic switch in cancers by oncogenes and tumor suppressor genes. *Science* 330: 1340–1344, 2010.
43. Li Y, Huang T, Carlson E, Melov S, Ursell P, Olson J, Noble L, Yoshimura M, Berger C, and Chan P. Dilated cardiomyopathy and neonatal lethality in mutant mice lacking manganese superoxide dismutase. *Nat Genet* 11: 376–381, 1995.
44. Low IC, Chen ZX, and Pervaiz S. Bcl-2 modulates resveratrol-induced ROS production by regulating mitochondrial respiration in tumor cells. *Antioxid Redox Signal* 13: 807–819, 2010.
45. Martin R, Ahn J, Nowell S, Hein D, Doll M, Martini B, and Ambrosone C. Association between manganese superoxide dismutase promoter gene polymorphism and breast cancer survival. *Breast Cancer Res* 8: R45, 2006.
46. Martinez B, Perez-Castillo A, and Santos A. The mitochondrial respiratory complex I is a target for 15-deoxy-delta12,14-prostaglandin J2 action. *J Lipid Res* 46: 736–743, 2005.
47. Mukhopadhyay S, Das SK, and Mukherjee S. Expression of Mn-superoxide dismutase gene in nontumorigenic and tumorigenic human mammary epithelial cells. *J Biomed Biotechnol* 4: 195–202, 2004.
48. Nishida S, Akai F, Iwasaki H, Hosokawa K, Kusunoki T, Suzuki K, Taniguchi N, Hashimoto S, and Tamura TT. Manganese superoxide dismutase content and localization in human thyroid tumours. *J Pathol* 169: 341–345, 1993.
49. Oberley TD. Mitochondria, manganese superoxide dismutase, and cancer. *Antioxid Redox Signal* 6: 483–487, 2004.
50. Oberley TD and Oberley LW. Antioxidant enzyme levels in cancer. *Histol Histopathol* 12: 525–535, 1997.
51. Oberley TD, Schultz JL, and Oberley LW. *In vitro* modulation of antioxidant enzyme levels in normal hamster kidney and estrogen-induced hamster kidney tumor. *Free Radic Biol Med* 16: 741–751, 1994.
52. Pacher P, Beckman JS, and Liaudet L. Nitric oxide and peroxynitrite in health and disease. *Physiol Rev* 87: 315–424, 2007.
53. Pelicano H, Carney D, and Huang P. ROS stress in cancer cells and therapeutic implications. *Drug Resist Updat* 7: 97–110, 2004.
54. Pelicano H, Feng L, Zhou Y, Carew JS, Hileman EO, Plunkett W, Keating MJ, and Huang P. Inhibition of mitochondrial respiration: a novel strategy to enhance drug-induced apoptosis in human leukemia cells by a reactive oxygen species-mediated mechanism. *J Biol Chem* 278: 37832–37839, 2003.
55. Pervaiz S and Clement MV. Tumor intracellular redox status and drug resistance—serendipity or a causal relationship? *Curr Pharm Des* 10: 1969–1977, 2004.
56. Pervaiz S and Clement MV. Superoxide anion: oncogenic reactive oxygen species? *Int J Biochem Cell Biol* 39: 1297–1304, 2007.
57. Prat A, Parker JS, Karginova O, Fan C, Livasy C, Herschkowitz JI, He X, and Perou CM. Phenotypic and molecular characterization of the claudin-low intrinsic subtype of breast cancer. *Breast Cancer Res* 12: R68, 2010.
58. Ray DM, Akbiyik F, and Phipps RP. The peroxisome proliferator-activated receptor gamma (PPARgamma) ligands 15-deoxy-Delta12,14-prostaglandin J2 and ciglitazone induce human B lymphocyte and B cell lymphoma apoptosis by PPARgamma-independent mechanisms. *J Immunol* 177: 5068–5076, 2006.
59. Shin SW, Seo CY, Han H, Han JY, Jeong JS, Kwak JY, and Park JI. 15d-PGJ2 induces apoptosis by reactive oxygen species-mediated inactivation of Akt in leukemia and colorectal cancer cells and shows *in vivo* antitumor activity. *Clin Cancer Res* 15: 5414–5425, 2009.
60. Soller M, Drose S, Brandt U, Brune B, and von Knethen A. Mechanism of thiazolidinedione-dependent cell death in Jurkat T cells. *Mol Pharmacol* 71: 1535–1544, 2007.
61. Tamai T, Uto H, Takami Y, Oda K, Saishoji A, Hashiguchi M, Kumagai K, Kure T, Mawatari S, Moriuchi A, Oketani M, Ido A, and Tsubouchi H. Serum manganese superoxide dismutase and thioredoxin are potential prognostic markers for hepatitis C virus-related hepatocellular carcinoma. *World J Gastroenterol* 17: 4890–4898, 2011.
62. Tontonoz P, Hu E, and Spiegelman BM. Regulation of adipocyte gene expression and differentiation by peroxisome proliferator activated receptor gamma. *Curr Opin Genet Dev* 5: 571–576, 1995.
63. Vaughn AE and Deshmukh M. Glucose metabolism inhibits apoptosis in neurons and cancer cells by redox inactivation of cytochrome c. *Nat Cell Biol* 10: 1477–1483, 2008.
64. Venkatachalam G, Kumar AP, Yue LS, Pervaiz S, Clement MV, and Sakharkar MK. Computational identification and experimental validation of PPRE motifs in NHE1 and MnSOD genes of human. *BMC Genomics* 10 Suppl 3: S5, 2009.
65. Verhaak RG, Hoadley KA, Purdom E, Wang V, Qi Y, Wilkerson MD, Miller CR, Ding L, Golub T, Mesirov JP, Alexe G, Lawrence M, O'Kelly M, Tamayo P, Weir BA, Gabriel S, Winckler W, Gupta S, Jakkula L, Feiler HS, Hodgson JG, James CD, Sarkaria JN, Brennan C, Kahn A, Spellman PT, Wilson RK, Speed TP, Gray JW, Meyerson M, Getz G, Perou CM, and Hayes DN. Integrated genomic analysis identifies clinically relevant subtypes of glioblastoma characterized by abnormalities in PDGFRA, IDH1, EGFR, and NF1. *Cancer Cell* 17: 98–110, 2010.
66. Virag L, Szabo E, Gergely P, and Szabo C. Peroxynitrite-induced cytotoxicity: mechanism and opportunities for intervention. *Toxicol Lett* 140–141: 113–124, 2003.

67. Wang J and Lu YY. Mitochondrial DNA 4977-bp deletion correlated with reactive oxygen species production and manganese superoxidedismutase expression in gastric tumor cells. *Chin Med J (Engl)* 122: 431–436, 2009.
68. Wang J and Yi J. Cancer cell killing via ROS: to increase or decrease, that is the question. *Cancer Biol Ther* 7: 1875–1884, 2008.
69. Ward PS and Thompson CB. Metabolic reprogramming: a cancer hallmark even warburg did not anticipate. *Cancer Cell* 21: 297–308, 2012.
70. Wenzel P, Schuhmacher S, Kienhofer J, Muller J, Hortmann M, Oelze M, Schulz E, Treiber N, Kawamoto T, Scharffetter-Kochanek K, Munzel T, Burkle A, Bachschmid MM, and Daiber A. Manganese superoxide dismutase and aldehyde dehydrogenase deficiency increase mitochondrial oxidative stress and aggravate age-dependent vascular dysfunction. *Cardiovasc Res* 80: 280–289, 2008.
71. Wink DA, Miranda KM, and Espey MG. Cytotoxicity related to oxidative and nitrosative stress by nitric oxide. *Exp Biol Med (Maywood)* 226: 621–623, 2001.

Address correspondence to:
Dr. Marie Véronique Clément
Department of Biochemistry
Yong Loo Lin School of Medicine
National University of Singapore
8 Medical Drive
Singapore 117597
Singapore

E-mail: bchmvc@nus.edu.sg

Date of first submission to ARS Central, March 10, 2013; date of final revised submission, August 1, 2013; date of acceptance, August 21, 2013.

Abbreviations Used

$15d\text{-}PGJ_2$ = 15-deoxy $^{\Delta12,14}$-PGJ_2
$CM\text{-}H_2DCFDA$ = 5-(and-6)-chloromethyl-2′,7′-dichlorodihydrofluorescein diacetate
ctsi = control scrambled siRNA
DNPPARγ = dominant negative peroxisome proliferator-activated receptor gamma
DOC = docetaxel
DOX = doxorubicin
FBS = fetal bovine serum
FeTPPS = 5,10,15,20-tetrakis(4-sulfonatophenyl) porphyrinato iron (III), chloride
GEO = gene expression omnibus
H_2O_2 = hydrogen peroxide
HR = hazard ratio
IHC = immunohistochemical
MnSOD = manganese superoxide dismutase
MTT = 3-(4,5-dimethylthiazol-2-yl)-2,5-diphenyltetrazolium bromide
NAC = N-acetyl cysteine
NO = nitric oxide
$O_2^{\bullet -}$ = superoxide anion
$^{\bullet}OH$ = hydroxyl radical
$ONOO^-$ = peroxynitrite
PBS = phosphate buffered saline
PMSF = phenylmethanesulfonyl fluoride
PPARγ = peroxisome proliferator-activated receptor gamma
PPRE = peroxisome proliferator response element
ROS = reactive oxygen species
siRNA = small-interfering ribonucleic acid
ssGSEA = single-sample geneset enrichment analysis
TCGA = the cancer genome atlas